Food Chemistry: X 22 (2024) 101487

Contents lists available at ScienceDirect

Food Chemistry: X

journal homepage: www.sciencedirect.com/journal/food-chemistry-x

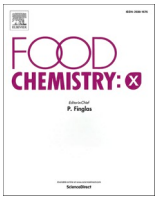

Comprehensive analysis of the dynamic changes of volatile and non-volatile metabolites in *boletus edulis* during processing by HS-SPME-GC–MS and UPLC-MS/MS analysis

Hao Yang [a,b,1], Weilan Li [a,b,1], Luxi Zi [a,b], Ningmeng Xu [a,b], Zhengyin Guo [b], Bangjie Chen [b], Yan Hua [a], Lei Guo [a,b,*]

[a] *The Key Laboratory of Forest Resources Conservation and Utilization in the Southwest Mountains of China Ministry of Education, Southwest Forestry University, Kunming, Yunnan, 650224, China*

[b] *College of Biological Science and Food Engineering, Southwest Forestry University, Kunming, Yunnan, 650224, China*

ARTICLE INFO

Chemical compounds studied in this article:
1-Octen-3-ol (PubChem CID: 18827)
(E)-2-Octenal (PubChem CID: 5283324)
2-Thiophenecarboxaldehyde (PubChem CID: 7364)
Methional (PubChem CID: 18635)
Linoleic acid (PubChem CID: 5280450)
Cysteine (PubChem CID: 5862)
Methionine (PubChem CID: 6137)
Glutamate acid (PubChem CID: 33032)

Keywords:
Boletus edulis
Drying
Enzyme activity
HS-SPME-GC–MS
UPLC-MS/MS

ABSTRACT

In order to investigate the dynamic changes of flavor compounds, Ultra Performance Liquid Chromatography Tandem Mass Spectrometry (UPLC-MS/MS) combined with Headspace Solid Phase Microextraction Gas Chromatography Mass Spectrometry (HS-SPME-GC–MS) was used to detect the metabolites in different drying processes. A total of 80 volatile compounds and 1319 non-volatile compounds were identified. The trend in the changes of C-8 compounds and sulfur-containing compounds were generally consistent with the trend of key enzyme activities. 479 differential metabolites were identified and revealed that metabolic profiles of compounds in *Boletus edulis* were altered with increased organic acids and derivatives and lipids and lipid-like molecules. Fatty acids and amino acids were transformed into volatile compounds under the action of enzymes, which played a significant role in the formation of the distinctive flavor of *Boletus edulis*. Our study provided a theoretical support for fully comprehending the formation mechanism of flavor from *Boletus edulis* during drying processes.

1. Introduction

Boletus edulis (*Boletus edulis* Bull. Fr.), commonly known as "porcini mushroom" or "king bolete", is a highly popular edible fungus renowned for its nutritional, flavorful, and pharmacological properties (Zhang et al., 2018). It is rich in carbohydrates, proteins, minerals, and flavor compounds, while containing fewer fats and calories (Tan, Zeng, & Xu, 2022). With the increasing awareness among consumers about the sensory quality of *Boletus edulis*, flavor has become an important factor influencing consumer choices. It is worth noting that fresh *Boletus edulis* is prone to spoilage and deterioration. Therefore, drying is often chosen as a method to extend the shelf life of *Boletus edulis* (Zhuang et al., 2020). The hot air drying method had a significant impact on the flavor formation and quality of *Boletus edulis*. (Zhang et al., 2023). Ren, Zheng, Zhao, Hu, and Yang (2022) conducted drying on *Coprinus comatus* by freeze-drying achieved the best texture properties, rehydration rate, and minimal colour change. Chen, Sheng, Wang, Chen, and Leng (2023) investigated the dynamic changes and correlations of 19 key volatile compounds, 20 amino acids, and 5 reducing sugars in the hot air drying process, and they discovered that Met (methionine) and ribose were precursors for the formation of dimethyl trisulfide from *Lentinus edodes*. Compared to fresh mushrooms, *Boletus edulis* produced a particularly enticing and strong aroma after drying, which increased the complexity of volatile compounds and gave them extremely high market value (Zhang et al., 2018). Therefore, elucidating the key aromatic compounds and their changes during the drying process of *Boletus edulis* is of special

* Corresponding author at: The Key Laboratory of Forest Resources Conservation and Utilization in the Southwest Mountains of China Ministry of Education, Southwest Forestry University, Kunming, Yunnan 650224, China
E-mail address: guolei@swfu.edu.cn (L. Guo).

[1] Contributed to this article equally and are co-first authors.

https://doi.org/10.1016/j.fochx.2024.101487
Received 22 April 2024; Received in revised form 16 May 2024; Accepted 16 May 2024
Available online 21 May 2024

significance.

The flavor components of mushrooms include volatile flavor compounds and non-volatile taste compounds. C-8 compounds and sulfur-containing compounds represent aroma components, while taste components mainly consist of organic acids, amino acids, nucleotides and peptides (Zhang et al., 2020). C-8 and sulfur-containing compounds are both produced through enzyme-catalyzed reactions. Lipoxygenase (LOX) and hydroperoxide lyase (HPL) catalyzed the formation of C-8 compounds from linoleic acid, such as 1-octen-3-one and 1-octen-3-ol (Tian, Zhao, Huang, Zeng, & Zheng, 2016). Meanwhile, γ-glutamyltranspeptidase (γ-GGT) and L-cysteine sulfoxide lyase (C—S lyase) catalyze the generation of sulfur compounds from vanillic acid (Zhang et al., 2021). Among these volatile compounds, 1-octen-3-ol, widely present in mushrooms, is a typical contributor to the mushroom-like aroma. However, there is currently limited research providing a comprehensive overview of the volatile components, non-volatile metabolites, and flavor differences of *Boletus edulis*. Therefore, to understand the contributions of different metabolite categories, consistent research is still needed for the identification and quantification of metabolites at different drying stages of *Boletus edulis*.

Metabolomic analysis based on UPLC-MS/MS boasts advantages such as high throughput, broad coverage, fast separation, and high sensitivity (Dong, Xian, Xiao, Zhu, & He, 2019). Furthermore, this technique is widely applied in the analysis of non-volatile component metabolites. Zhao et al. (2022) determined toxins in mushroom and urine samples using UPLC-MS/MS, and discovered that cooked mushrooms and their broth served as valuable materials for identifying mushroom poisoning caused by mushroom toxins. Zhang et al. (2023) detected 631 non-volatile compounds and 242 volatile compounds, and the results indicated that the flavor differences between the two varieties were highly correlated with the content of lipids, carbohydrates, amino acids and their derivatives, alcohols. In the present study, the dynamic changes of volatile and non-volatile compounds of *Boletus edulis* under different drying stages were comprehensively explored by combining HS-SPME-GC–MS and UPLC-MS/MS, and aiming to elucidate the correlation between enzyme activity and the production of volatile compounds. Moreover, the Metabolism pathway of key aromatic compounds was explored preliminary. These findings can provide useful evidence for elucidating the flavor and metabolite differences of *Boletus edulis* under different drying processes and for further studies.

2. Materials and methods

2.1. Mushroom preparation

Fresh *Boletus edulis* were purchased from Jinning (Kunming, China) on August 26, 2023. The fresh fruit bodying was cleaned and selected for further experimental use. The fresh *Boletus edulis* were evenly laid flat on trays and dried with an Electro thermostatic blast oven (Experimental Instrument Factory, Shanghai, China) at 60 °C. The drying time were set at 0 h, 1 h, 3 h, 5 h, 7 h and 9 h, respectively (Fig. 1). After drying, the enzyme activity was determined immediately. Meanwhile, the different sample were dried by a vacuum freeze dryer (Shanghai Yetuo Technology Co., LTD, Shanghai, China) for further analysis, respectively. The vacuum degree was 2 Pa and the cold trap temperature was −60 °C. The freeze-dried *Boletus edulis* were ground and sieved using an 80-mesh sieve.

2.2. Volatile components analysis

The HS-SPME was used for extraction of volatile components in *Boletus edulis* according to the method of Li et al. (2023). Precisely, 0.50 g dried samples were added into the headspace bottle, and 1-decanol was added as the internal standard. A 50/30 μm DVB/CAR/PDMS extraction fiber was inserted into the headspace bottle and the extraction conditions were as follows: each sample was equilibrated at 79 °C for 28 min and then extraction was performed using a fiber head for 23 min at 79 °C. After that, the fiber was immediately inserted into the injector of the GC–MS and desorption at 250 °C for 15 min.

The volatile components were separated and detected using HP-5MS chromatographic columns (30 m × 0.25 mm, 0.25 μm) by GC–MS. The splitless mode was used for each injection. The initial temperature was set at 40 °C and maintained for 5 min. It was then ramped up at a rate of 5 °C per minute until reaching 260 °C, where it was held for 2 min. Pure helium was used as carrier gas with a flow rate of 1.00 mL/min. Electron ionization energy was recorded as 70 eV, the ion source temperature was 230 °C, and the transfer line temperature was set at 250 °C. A full scan mode was operated at a quadrupole temperature of 150 °C. The scan ranges were *m/z* 30–400. The volatile components were compared with the National Institute of Standards and Technology mass spectrum library 14.0 (NIST library14.0). The match scores of the compounds were

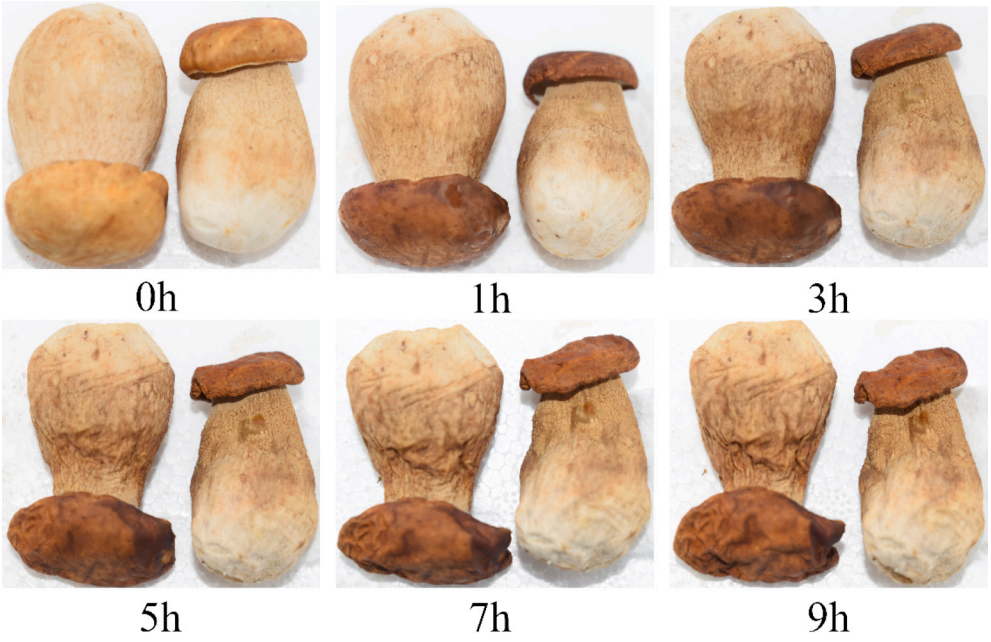

Fig. 1. The phenotype of *Boletus edulis* at the drying time of 0 h, 1 h, 3 h,5 h, 7 h and 9 h, respectively.

higher than 80%. The relative content (C) of volatile components was calculated by the following eq. (1):

$$C = \frac{S_1 \times m_2}{S_2 \times m_1} \quad (1)$$

where S_1 is the peak area of volatile components, and S_2 is the peak area of internal standard. m_1 and m_2 are the weight of sample and weight of internal markers, respectively.

The compound retention index was calculated by the following eq. (2) (Niu, Tian, & Zhan, 2022):

$$RI = 100 \times \left(n + \frac{t - t_n}{t_{(n+1)} - t_n}\right) \quad (2)$$

where *RI* is the retention index of the component to be tested. *tn* and *t(n + 1)* are the retention time of n-alkanes immediately before and after compound to be tested. *N* is the number of carbon atoms of n-alkanes; *t* is the retention time of component to be tested.

2.3. Synthetase activity assay

Synthetase activity assay kits (Suzhou Michy Biomedical Technology Co., Ltd) were used for LOX, alcohol dehydrogenase (ADH), γ-GGT and C—S lyase extraction and assays. LOX and ADH were involved in the synthesis pathway of C-8 compounds, while γ-GGT and C—S lyase were participated in the synthesis pathway of sulfur-containing compounds. LOX catalyzed the production of peroxides from linoleic acid and linolenic acid (Li, Yang, Li, Chen, & Liu, 2023). The enzyme activity of LOX could be calculated by measuring the rate of increase in absorbance at 234 nm as the formula:

$$E(LOX) = \frac{820^{*}\Delta A}{W} \quad (3)$$

where ΔA is the difference in absorbance between the experimental group and the control group. *W* is the weight of sample.

ADH played a crucial role in many physiological processes, as it could catalyze the reversible conversion between ethanol and acetaldehyde (Sun et al., 2021). The enzyme activity of ADH could be calculated by measuring the decrease in absorbance at 340 nm as the formula:

$$E(ADH) = \frac{1608^{*}\Delta A}{W} \quad (4)$$

where ΔA is the difference in absorbance between the experimental group and the control group. *W* is the weight of sample.

γ-GGT catalyzed the transfer of the γ-glutamyl group from γ-glutamyl-p-nitroanilide to *N*-acetylglycine, producing p-nitroaniline in the past. The enzyme activity of γ-GGT could be calculated by measuring the increase in absorbance at 405 nm as the formula:

$$E(\gamma GGT) = \frac{1.67^{*}(\Delta A - 0.0016)}{W} \quad (5)$$

where ΔA is the difference in absorbance between the experimental group and the control group. *W* is the weight of sample.

C—S lyase catalyzed the production of pyruvate from cysteine. This pyruvate reacted with 2,4-dinitrophenylhydrazine in an alkaline environment. The enzyme activity of C—S lyase could be calculated by measuring the increase in absorbance at 510 nm as the formula:

$$E(CSL) = \frac{0.116^{*}(\Delta A - 0.0023)}{W} \quad (6)$$

where ΔA is the difference in absorbance between the experimental group and the control group. *W* is the weight of sample.

2.4. Non-volatile compounds analysis

2.4.1. Quality control analysis

The mixed sample of six samples as a quality control (QC) sample was used to monitor the reproducibility of the assay. During the instrumental analysis, QC sample was analyzed every three test samples.

2.4.2. Pretreatment method

Sample pretreatment was carried out according to the method of Tu et al. (2023). The sample was thawed at 4 °C, ground in liquid nitrogen, and 80 mg of the sample was weighed into an EP tube. Three medium-sized steel beads were added along with 200 μL pre-cooled methanol solution (80%). The mixture was homogenized in a tissue homogenizer, followed by the addition of 800 μL pre-cooled methanol solution (80%). The sample was sonicated in an ice bath for 20 min, then allowed to stand at −20 °C for 1 h. After centrifugation at 16000*g* for 20 min at 4 °C, the supernatant was collected, and the supernatant was evaporated using a high-speed vacuum concentrator.

For mass spectrometry detection, 100 μL methanol solution (50%) was added for reconstitution. After centrifugation at 20000*g* for 15 min at 4 °C, the supernatant was collected for the further analysis.

2.4.3. UPLC-MS/MS analysis

UPLC-MS/MS analysis was performed using the method proposed by Zhang et al. (2023) with slight modifications. Throughout the entire analysis process, the samples were placed in a 4 °C automatic injector. The samples were analyzed using the SHIMADZU-LC30 Ultra High-Performance Liquid Chromatography (UPLC) system with a 2.1 × 100 mm, 1.8 μm column (Waters, Milford, MA, USA). The injection volume was 4 μL, column temperature was set at 40 °C, and the flow rate was 0.3 mL/min. The chromatographic mobile phase consisted of A: 0.1% formic acid aqueous solution and B: acetonitrile. The chromatographic gradient elution program was as follows: 0–2 min, 0% B; 2–6 min, B linearly increased from 0% to 48%; 6–10 min, B linearly increased from 48% to 100%; 10–12 min, B maintained at 100%; 12–12.1 min, B linearly decreased from 100% to 0%; 12.1–15 min, B maintained at 0%.

Each sample was subjected to electrospray ionization (ESI) for detection in both positive ion (+) and negative ion (−) modes. Following separation by UPLC, mass spectrometric analysis was conducted using a QE Plus mass spectrometer (Thermo Scientific) with heated electrospray ionization (HESI) source. The ionization conditions were set as follows: Spray Voltage: 3.8 kV (+) and 3.2 kV (−); Capillary Temperature: 320 (±); Sheath Gas: 30 (±); Aux Gas: 5 (±); Probe Heater Temp: 350 (±); S-Lens RF Level: 50.

The mass spectrometric acquisition settings were configured as follows: Mass Spectrometry Acquisition Time: 15 min; Full scan range for precursor ions: 75–1050 *m/z*; Primary mass spectrometry resolution: 70,000 @ m/z 200; AGC (Automatic Gain Control) target: 3e6; Primary Maximum Ion Trap (IT) time: 100 ms. For the secondary mass spectrometry analysis, the following method was employed: After each full scan, 10 of the highest intensity precursor ions were selected for MS2 scan. The secondary mass spectrometry resolution was set at 17,500 @ m/z 200; AGC target: 1e5; Secondary Maximum IT: 50 ms; MS2 Activation Type: HCD (Higher Energy Collision Dissociation); Isolation window: 2 m/z; Normalized collision energy (Stepped): 20, 30, 40.

2.4.4. Metabolomics data processing

The data were processed using the MSDIAL software for peak alignment, retention time correction, and peak area extraction. Metabolite structural identification was conducted through accurate mass matching (mass tolerance <10 ppm) and MS/MS spectrum matching (mass tolerance <0.01 Da). Public databases such as HMDB, MassBank, GNPS, and a self-established library of metabolite standards (BP-DB) were searched for identification. Total peak area normalization was performed separately for positive and negative ion data.

2.5. Statistical analysis

All samples were measured three times in parallel and the data were expressed as mean ± standard deviation. ANOVA analysis of variance was performed by SPSS 26.0 software. The experimental Origin 2021 and SIMCA 14.1 was used for PCA and OPLS-DA analysis. Heatmap clustering analysis was performed using TBtools. $P \leq 0.05$ was considered a significant difference and $P \leq 0.01$ was recognized as an extremely significant difference.

3. Results and discussion

3.1. The volatile metabolites profile of boletus edulis at different drying stages

3.1.1. Volatile components analyzed

A total of 80 volatile components were detected by HS-SPME/GC–MS, which were classified into 6 categories, including 6 alkanes, 8 alcohols, 13 aldehydes, 13 esters, 19 ketones and 21 other compounds. The detailed information of volatile components was shown in Table 1. The variable was considered to play an important role when VIP exceeded 1 (Wang et al., 2022). In this study, 19 compounds with VIP > 1 were screened out, which were mainly aldehydes, ketones and alcohols. Eleven C-8 compounds and three sulfur-containing compounds were detected by HS-SPME/GC–MS. Among them, the VIP of (E)-2-octen-1-ol (3.03), 1-octen-3-ol (2.65), acetophenone (2.09), (E)-2-octenal (1.91), benzeneacetaldehyde (1.64), 1-octen-3-one (1.22), phenylethyl alcohol (1.15) and 2-thiophenecarboxaldehyde (1.13) were all exceeded 1. These compounds made significant contributions to the flavor profile of *Boletus edulis* at different drying stages. As shown in Fig. 2A, the three component types with higher proportions were alcohols (37.4%), ketones (25.2%) and aldehydes (19.1%). In addition, the contents of volatile component categories varied among different drying stages, shown in Fig. 2B. To be specific, it was observed that the percentage of alcohols decreased by 46% after extending the drying time to 9 h, which may be attributed to the abundant presence of alcohols in fresh edible mushrooms. Due to the high volatility and instability of alcohols, the contents of alcohols significantly decreased with prolonged drying time. 1-octen-3-ol, which was imparted the distinctive “earthy” and “mushroom-like” odor to *Boletus edulis*, and was formed due to the oxidation and enzymatic degradation of linoleic acid. After 3 h of drying, the aldehydes percentage reached 24%. In addition, the percentage of ketones peaked at 48% at the drying time of 9 h. There was a significant upward trend in others during the drying process. This could be attributed to the presence of numerous Maillard reaction products in these compounds, including pyrazines, furans, and sulfur-containing compounds (Shakoor, Zhang, Xie, & Yang, 2022). It is worth mentioning that 3-decen-2-one was detected in each drying stage, and its VIP exceeded 1. 3-decen-2-one stands as a pivotal volatile compound liberated in the oxidation reaction of unsaturated fatty acids. These compounds assumed a substantial role within these biochemical processes, imparting distinct flavor traits to the particular scents of *Boletus edulis.*

An upset diagram was used to identify common and unique differential volatile compounds among the different samples. As shown in Fig. 2C, the largest number of volatile compounds (69) and the smallest number of volatile compounds (40) were detected at the drying time of 9 h and 0 h, respectively. 26 volatile compounds were detected at each drying stage, predominantly comprising esters, alkanes, and ketones, such as 2-ethylhexyl salicylate, dibutyl phthalate, 3-decen-2-one, 2-undecanone and benzaldehyde. There was a notable difference in volatile compounds between short-term drying (0−2*h*) and long-term drying (7–9 h). This difference in volatile compounds was primarily attributed to the Maillard reaction products, such as 3-ethyl-2,5-dimethyl-pyrazine, 3-phenyl-furan, 3-phenyl-pyridine, 2-methyl-1H-Pyrrole. The observed distinction was attributed to the fact that, with prolonged drying time, aldehydes and amines underwent condensation reactions to yield pyrroles, whereas esters underwent condensation reactions to form furans (Cebi, 2021; Magalhães et al., 2023).

3.1.2. The volatile components analyzed by PCA

In order to better examine the regularity of variation in volatile compounds during the drying process. The volatile chemical components obtained were processed using PCA, and the result was shown in Fig. 2D and Fig. 2E. The R2X [1] = 0.492 and the R2X [2] = 0.18, indicating that the model samples have good reliability. It could be observed that there was a good distinction at the drying time of 9 h, and the differences between different groups were also noticeable. The two samples (7 h and 9 h) were located on the left side, and the volatile compounds contained 2-thiophenecarboxaldehyde, methional, dodecane, 2-ethyl-6-methyl-pyrazine etc. Three samples (1 h, 3 h and 5 h) were located in the right area, and the volatile compounds contained 1-octen-3-ol, (E)-2-octenal, hexanal, decanal, phenylethyl alcohol, etc. This phenomenon could be ascribed to the generation of numerous other volatile compounds during the extended drying process. As shown in Fig. 2F, 200 permutation analyses were conducted on all experimental data to validate the existence of the model. The intercept between the Q2 regression line was <0, proving that the model was reliable. And there was no overfitting, proving that the analysis was effective. (R2 = 0.71, Q2 = −5.25).

3.1.3. Enzymatic activity analysis of flavor synthesis key enzymes

Flavor synthesis enzymes such as LOX, ADH, γ-GGT, and C—S lyase participate in the biosynthetic pathway of characteristic aroma compounds in *Boletus edulis*. C-8 compounds were primarily formed through the consecutive catalytic hydrolysis of linoleic acid and linolenic acid by LOX and HPL. Ketones were further catalyzed into alcohols by ADH. Sulfur-containing compounds were formed by the hydrolysis of cysteine to produce lentinic acid by γ-GGT, which was then further catalyzed by C—S lyase to undergo elimination and substitution reactions (Qi et al., 2020). This contributes to the formation of precursors and aromatic components, enhancing the overall flavor profile of *Boletus edulis*. As shown in Fig. 3A, the categories and contents of C-8 compounds and sulfur-containing compounds were assessed at various stages of the drying process. The content of (E)-2-octen-1-ol reached its peak (955.62 ± 2.35 μg/Kg) at the drying time of 5 h. The formation of (E)-2-octen-1-ol was catalyzed by LOX and ADH after lipids were hydrolyzed into free fatty acids by acetyl hydrolase, and it intimately intertwined with the aromatic essence of fresh fruity and vegetal (Sun, Zhang et al., 2020). This compound assumed a substantial role within these biochemical processes, imparting distinct flavor traits to the particular scents of *Boletus edulis*. Considering the enzyme activity, it can be observed that the variation trend in the contents of C-8 compounds aligned closely with the variations in enzyme activities of LOX and ADH. Similarly, the variation trend of sulfur-containing compound contents during the drying process was generally consistent with the changes in enzyme activities of γ-GGT and C—S lyase. As shown in Fig. 3B, the enzymatic activities of LOX and ADH reached their respective maximum values at 3 h and 5 h. With extended drying time, the enzymatic activities of LOX and ADH displayed a trend of initial increase followed by a decrease. Combining the results from HS-SPME/GC–MS, it was observed that there was a secondary activation and elevation in enzyme activity of LOX at the drying time of 7 h. This was because the drying led to a sudden increase in the external temperature of *Boletus edulis*, causing internal disruption in the organism and consequently a decrease in enzyme activity. As the drying time prolongs, the organism adapted to the environment, restoring internal balance, and resulting in the thermal activation of enzymes. It was speculated that at 3 h and 5 h of drying, reactions were initiated by LOX and ADH resulting primarily in the production of alcohols, aldehydes, and ketones. Among these compounds, (E)-2-octen-1-ol, and 1-octen-3-ol had the highest concentrations, representing characteristic flavor compounds of *Boletus edulis* and imparting a mushroom-like taste. It was noteworthy that the enzyme

Table 1
The volatile compounds of *Boletus edulis* at different drying stages.

No.	Classification	CAS	Compounds	Formula	Content (μg/kg)						Identification Method	RT	RI [a]	RI [b]	Odor description	VIP
					0 h	1 h	3 h	5 h	7 h	9 h						
1	**Alcohols**	3391-86-4	1-Octen-3-ol	$C_8H_{16}O$	443.92 ± 3.76^{d}	35.97 ± 4.06^{e}	656.15 ± 4.36^{a}	592.57 ± 4.66^{b}	581.8 ± 3.96^{c}	18.92 ± 2.16^{f}	MS/RI	12.45	1035.78	1012	mushroom, earthy, green, chicken	2.65
2		143–08-8	1-Nonanol	$C_9H_{20}O$	22.03 ± 3.01^{a}	14.12 ± 3.31^{b}	8.76 ± 3.61^{d}	6.96 ± 1.91^{e}	11.11 ± 3.21^{c}	11.00 ± 1.41^{c}	MS/RI	18.63	1068.85	1169	fatty, floral, rose, orange, dusty	0.44
3		60_12_8	Phenylethyl Alcohol	$C_8H_{10}O$	183.76 ± 4.23^{a}	130.6 ± 4.53^{c}	129.40 ± 4.83^{c}	76.9 ± 5.13^{d}	129.83 ± 4.43^{c}	152.88 ± 2.63^{b}	MS/RI	16.82	1109.94	1111	Sweet, floral, bready, rose	1.15
4		77–53-2	Cedrol	$C_{15}H_{26}O$	86.57 ± 3.23^{a}	60.57 ± 3.53^{c}	52.57 ± 3.83^{d}	48.93 ± 4.13^{e}	51.79 ± 3.43^{d}	77.82 ± 1.63^{b}	MS/RI	29.98	1601.19	1599	cedarwood, sweet	0.76
5		18,409–17-1	(E)-2-Octen-1-ol	$C_8H_{16}O$	323.20 ± 1.45^{d}	131.83 ± 1.75^{e}	758.83 ± 2.05^{b}	955.62 ± 2.35^{a}	685.83 ± 1.65^{c}	–	MS/RI	15.43	1067.67	1069	green, citrus, vegetable, fatty	3.03
6		4602-84-0	Farnesyl alcohol	$C_{15}H_{26}O$	14.38 ± 4.78^{c}	27.88 ± 5.08^{a}	9.40 ± 1.38^{e}	6.84 ± 1.68^{d}	22.26 ± 4.98^{b}	21.07 ± 3.18^{b}	MS/RI	32.55	1716.16	1721	mild, fresh, sweet, floral	0.64
7		589–98-0	3-Octanol	$C_8H_{18}O$	12.08 ± 2.45^{b}	14.95 ± 2.75^{a}	–	–	–	–	MS/RI	12.94	1079.77	1013	earthy, mushroom, herbal, melon, woody	0.50
8		40,716–66-3	*E*-Nerolidol	$C_{15}H_{26}O$	–	–	4.40 ± 0.61^{d}	11.82 ± 3.91^{b}	11.75 ± 3.21^{b}	23.88 ± 1.41^{a}	MS/RI	29.00	1632.77	1571	floral, green, citrus, woody, waxy	0.54
9	**Aldehydes**	112–31-2	Decanal	$C_{10}H_{20}O$	74.64 ± 1.34^{a}	35.18 ± 1.64^{c}	37.26 ± 1.94^{b}	28.83 ± 2.24^{d}	34.82 ± 1.54^{c}	7.34 ± 0.74^{e}	MS/RI	19.63	1201.56	1200	sweet, waxy, citrus, floral	0.88
10		122–78-1	Benzeneacetaldehyde	C_8H_8O	208.83 ± 4.45^{a}	62.79 ± 4.75^{e}	97.40 ± 5.05^{c}	79.05 ± 5.35^{d}	125.12 ± 4.65^{b}	72.91 ± 2.85^{f}	MS/RI	14.50	1039.98	1043	sweet, floral, honey, cocoa	1.64
11		100–52-7	Benzaldehyde	C_7H_6O	88.94 ± 2.34^{d}	31.52 ± 2.64^{e}	110.92 ± 2.94^{b}	105.96 ± 3.24^{c}	186.33 ± 2.54^{a}	109.74 ± 0.74^{b}	MS/RI	11.57	989.12	966	sweet, almond, cherry	1.24
12		124–19-6	Nonanal	$C_9H_{18}O$	33.81 ± 3.67^{b}	13.93 ± 3.97^{d}	30.97 ± 4.27^{c}	31.99 ± 4.57^{c}	46.98 ± 3.87^{a}	–	MS/RI	16.54	1100.67	1102	waxy, rose, orris, orange, peel, fatty,	0.75
13		4411-89-6	2-Phenyl-2-butenal	$C_{10}H_{10}O$	38.59 ± 1.01^{d}	22.04 ± 1.31^{e}	146.69 ± 1.61^{a}	92.04 ± 1.91^{c}	126.08 ± 1.21^{a}	96.73 ± 0.41^{b}	MS/RI	21.55	1269.16	1268	sweet, honey, cocoa, nutty, radish	1.50
14		5910-87-2	2,4-Nonadienal	$C_9H_{14}O$	13.63 ± 4.23^{a}	5.91 ± 1.53^{c}	7.31 ± 0.83^{c}	11.34 ± 4.13^{b}	–	–	MS/RI	19.87	1135.88	1214	fatty, waxy, cucumber, fruit, chicken	0.58
15		2548-87-0	(E)-2-Octenal	$C_8H_{14}O$	70.65 ± 1.56^{c}	65.47 ± 1.86^{c}	227.51 ± 2.16^{a}	150.07 ± 2.46^{b}	32.99 ± 1.76^{d}	–	MS/RI	15.02	1055.33	1056.7	cucumber, fatty, herbal, banana	1.91
16		3268-49-3	Methional	C_4H_8OS	23.39 ± 4.01^{c}	8.21 ± 2.31^{d}	20.44 ± 4.61^{c}	26.81 ± 4.91^{c}	53.74 ± 4.21^{b}	62.87 ± 2.41^{a}	MS/RI	9.63	905.62	906	earthy, vegetable, creamy	0.74
17		111–71–7	Heptanal	$C_7H_{14}O$	–	5.62 ± 0.97^{d}	21.47 ± 2.27^{a}	15.58 ± 2.57^{c}	18.97 ± 1.87^{b}	4.6 ± 1.07^{d}	MS/RI	9.50	899.88	901	fatty, green, herbal, wine-lee	0.63
18		98–03-3	2-Thiophenecarboxaldehyde	C_5H_4OS	–	2.93 ± 0.42^{e}	12.33 ± 1.72^{d}	27.64 ± 2.02^{c}	95.96 ± 1.32^{a}	88.75 ± 0.52^{b}	MS/RI	13.09	1092.80	1026	sulfurous	1.13
19		19,780–25-7	2-ethyl-2-Butenal	$C_6H_{10}O$	–	–	4.78 ± 1.27^{b}	3.61 ± 0.57^{c}	10.68 ± 2.87^{a}	4.09 ± 1.07^{c}	MS/RI	6.88	828.57	808	N	0.42
20		21,834–92-4	5-Methyl-2-phenyl-2-hexenal	$C_{13}H_{16}O$	–	–	–	–	33.39 ± 4.09^{b}	50.43 ± 2.29^{a}	MS/RI	27.26	1474.66	1483	nut, sweet, chocolate, fruity	0.77

(*continued on next page*)

Table 1 (*continued*)

No.	Classification	CAS	Compounds	Formula	Content (μg/kg)						Identification Method	RT	RI [a]	RI [b]	Odor description	VIP
					0 h	1 h	3 h	5 h	7 h	9 h						
21		498–60-2	3-Furaldehyde	$C_5H_4O_2$	–	–	–	–	8.81 ± 1.76^{b}	13.09 ± 0.96^{a}	MS/RI	6.98	831.05	831.7	N	0.40
22	**Esters**	118–60-5	2-Ethylhexyl salicylate	$C_{15}H_{22}O_3$	227.35 ± 2.34^{a}	49.7 ± 3.64^{d}	42.76 ± 3.94^{e}	37.25 ± 4.24^{f}	85.32 ± 3.54^{b}	62.86 ± 1.74^{c}	MS/RI	34.37	1801.49	1816.7	orchid, sweet, balsamic	1.62
23		118–56-9	Homosalate	$C_{16}H_{22}O_3$	30.93 ± 4.56^{a}	15.01 ± 4.86^{b}	4.80 ± 1.16^{b}	4.45 ± 0.46^{b}	9.54 ± 1.76^{c}	6.52 ± 1.96^{d}	MS/RI	35.50	1857.18	1903	mild, menthol	0.57
24		84–69-5	Diisobutyl phthalate	$C_{16}H_{22}O_4$	100.14 ± 2.56^{a}	23.79 ± 2.86^{c}	27.33 ± 3.16^{c}	29.13 ± 3.46^{c}	47.67 ± 2.76^{b}	41.59 ± 0.96^{b}	MS/RI	35.60	1861.99	1869	N	1.10
25		84–74-2	Dibutyl phthalate	$C_{16}H_{22}O_4$	47.25 ± 3.45^{b}	25.22 ± 3.75^{c}	35.22 ± 4.05^{c}	37.63 ± 4.35^{c}	49.47 ± 3.65^{a}	47.4 ± 1.85^{b}	MS/RI	37.45	1987.78	1968.4	faint odor	0.52
26		77–90-7	Tributyl acetylcitrate	$C_{20}H_{34}O_8$	11.34 ± 1.23^{b}	2.73 ± 0.53^{d}	9.95 ± 1.83^{c}	4.40 ± 0.13^{d}	24.82 ± 1.43^{a}	9.46 ± 0.63^{c}	MS/RI	42.92	2089.30	2224	very faint, herbal, wine, sweet	0.65
27		544–35-4	Linoleic acid ethyl ester	$C_{20}H_{36}O_2$	7.25 ± 1.67^{d}	–	2.58 ± 0.27^{e}	6.02 ± 1.57^{c}	54.37 ± 4.87^{a}	48.22 ± 3.07^{b}	MS/RI	41.10	2054.13	2144	fatty, fruity, oily	0.90
28		131–11-3	Dimethyl phthalate	$C_{10}H_{10}O_4$	7.91 ± 1.23^{e}	5.55 ± 0.53^{d}	10.20 ± 2.83^{c}	16.14 ± 3.13^{b}	10.69 ± 2.43^{c}	23.45 ± 0.63^{a}	MS/RI	26.38	1451.20	1466.2	N	0.58
29		84–66-2	Diethyl Phthalate	$C_{12}H_{14}O_4$	5.65 ± 1.89^{a}	3.03 ± 0.19^{d}	3.89 ± 0.49^{e}	4.38 ± 0.79^{c}	4.76 ± 0.09^{b}	–	MS/RI	29.74	1673.51	1597	N	0.26
30		6846-50-0	2,2,4-Trimethyl-1,3-pentanediol diisobutyrate	$C_{16}H_{30}O_4$	5.17 ± 1.67^{b}	5.30 ± 0.97^{a}	–	–	–	–	MS/RI	23.72	1382.96	1587.5	N	0.31
31		123–66-0	Ethyl caproate	$C_8H_{16}O_2$	27.64 ± 3.89^{a}	20.78 ± 4.19^{b}	–	–	–	–	MS/RI	18.98	1180.29	1007	sweet, fruity, pineapple, waxy	0.68
32		103–23-1	Diethylhexyl adipate	$C_{22}H_{42}O_4$	–	13.8 ± 1.53^{b}	14.87 ± 1.83^{a}	14.46 ± 2.13^{a}	7.64 ± 1.43^{c}	4.24 ± 0.63^{d}	MS/RI	45.09	2390.44	2398	N	0.48
33		83,834–59-7	2-Ethylhexyl trans-4-methoxycinnamate	$C_{18}H_{26}O_3$	–	–	–	2.63 ± 0.79^{a}	2.24 ± 0.09^{b}	1.91 ± 0.29^{c}	MS/RI	43.83	2319.91	2339	N	0.26
34		112–39-0	n-Hexadecanoic acid methyl ester	$C_{17}H_{34}O_2$	–	–	–	–	8.07 ± 1.21^{a}	7.19 ± 0.41^{b}	MS/RI	36.72	1928.25	1928.1	oily, waxy, fatty, orris	0.30
35	**Alkanes**	3891-99-4	2,6,10-Trimethyltridecane	$C_{16}H_{34}$	11.81 ± 1.78^{d}	12.28 ± 2.08^{d}	14.11 ± 2.38^{d}	27.59 ± 2.68^{a}	21.14 ± 1.98^{b}	19.61 ± 1.18^{c}	MS/RI	26.51	1456.63	1465.1	N	0.59
36		3891-98-3	2,6,10-Trimethyldodecane	$C_{15}H_{32}$	6.70 ± 4.67^{d}	6.11 ± 1.97^{d}	5.25 ± 1.27^{d}	12.31 ± 5.57^{a}	10.33 ± 4.87^{b}	11.31 ± 3.07^{c}	MS/RI	24.34	1500.36	1382	N	0.46
37		61,141–72-8	4,6-dimethyl-Dodecane	$C_{14}H_{30}$	4.65 ± 1.89^{d}	4.69 ± 0.19^{d}	8.09 ± 0.49^{c}	8.35 ± 1.79^{b}	13.29 ± 3.09^{a}	7.70 ± 1.29^{d}	MS/RI	23.01	1336.97	1325	N	0.35
38		2882-96-4	3-methyl-Pentadecane	$C_{16}H_{34}$	5.17 ± 1.78^{e}	2.12 ± 0.08^{c}	3.12 ± 0.38^{d}	4.28 ± 0.68^{d}	6.51 ± 0.98^{a}	6.28 ± 0.18^{b}	MS/RI	29.12	1600.75	1571	N	0.26
39		17,301–30-3	3,8-dimethyl-Undecane	$C_{13}H_{28}$	3.12 ± 0.89^{c}	4.87 ± 0.19^{c}	3.21 ± 0.49^{d}	24.10 ± 2.79^{a}	5.06 ± 0.09^{b}	–	MS/RI	23.52	1369.96	1228	N	0.87
40		18,435–22-8	3-methyl-Tetradecane	$C_{15}H_{32}$	2.37 ± 0.01^{a}	2.15 ± 4.31^{a}	–	–	–	–	MS/RI	26.71	1464.75	1468	N	0.21
41	**Ketones**	98–86-2	Acetophenone	C_8H_8O	25.9 ± 2.12^{c}	267.47 ± 2.13^{c}	43.76 ± 3.91^{c}	20.46 ± 3.21^{a}	27.90 ± 1.41^{c}	44.87 ± 3.23^{ab}	MS/RI	15.27	1062.72	1065	sweet, hawthorn, mimosa, almond	2.09
42		112–12-9	2-Undecanone	$C_{11}H_{22}O$	42.44 ± 3.01^{a}	18.19 ± 5.57^{d}	46.28 ± 2.24^{c}	78.13 ± 1.54^{c}	124.15 ± 0.74^{b}	187.09 ± 1.45^{a}	MS/RI	22.14	1289.87	1291	fruity, creamy, floral	1.28
43		10,519–33-2	3-Decen-2-one	$C_{10}H_{18}O$	16.57 ± 1.45^{e}	45.83 ± 3.13^{d}	125.59 ± 5.35^{c}	422.38 ± 4.65^{b}	403.62 ± 2.85^{b}	100.89 ± 4.78^{a}	MS/RI	20.64	1237.01	1233	fatty, green, apple, earthy	2.60
44		3796-70-1	(*E*)-Geranylacetone	$C_{13}H_{22}O$	32.10 ± 4.34^{d}	20.70 ± 4.79^{d}	35.25 ± 3.24^{c}	51.01 ± 2.54^{c}	134.79 ± 0.74^{b}	170.76 ± 2.45^{a}	MS/RI	26.31	1448.43	1452	fruity, rose, woody	1.29
45		106–68-3	3-Octanone	$C_8H_{16}O$	11.10 ± 2.34^{a}	6.74 ± 1.57^{b}	–	–	–	–	MS/RI	12.61	1050.45	998	herbal, lavender,	0.42

(*continued on next page*)

Table 1 (*continued*)

No.	Classification	CAS	Compounds	Formula	Content (μg/kg)						Identification Method	RT	RI [a]	RI [b]	Odor description	VIP
					0 h	1 h	3 h	5 h	7 h	9 h						
46		4312–99-6	1-Octen-3-one	$C_8H_{14}O$	38.04 ± 4.67^{b}	31.16 ± 4.79^{c}	76.45 ± 1.91^{a}	39.02 ± 1.21^{b}	–	16.74 ± 1.34^{d}	MS/RI	12.30	1022.50	983	sweet, mushroom herbal, mushroom, earthy	1.22
47		110–43-0	2-Heptanone	$C_7H_{14}O$	–	2.66 ± 0.13^{c}	–	4.18 ± 0.43^{c}	–	3.11 ± 0.45^{a}	MS/RI	9.11	889.40	889	fruity, sweet, coconut, woody	0.43
48		1669-44-9	3-Octen-2-one	$C_8H_{14}O$	–	–	–	–	2.71 ± 0.96^{b}	5.83 ± 0.34^{a}	MS/RI	14.42	1037.48	1037	earthy, mushroom, hay, blueberry	0.24
49		22,047–26-3	1-(6-Methyl-2-pyrazinyl)-1-ethanone	$C_7H_8N_2O$	–	–	–	–	12.00 ± 2.41^{b}	39.19 ± 3.67^{a}	MS/RI	16.98	1115.19	1095	roasted, coffee, cocoa, popcorn	0.61
50		28,564–83-2	2,3-dihydro-3,5-dihydroxy-6-methyl-4(4H)-pyranone	$C_6H_8O_4$	–	–	–	–	427.12 ± 1.07^{b}	761.70 ± 1.01^{a}	MS/RI	17.89	1144.68	1149	N	2.80
51		104–61-0	(3H)-Dihydro-5-pentyl-2-furanone	$C_9H_{16}O_2$	–	–	–	–	45.81 ± 0.52^{b}	26.53 ± 4.23^{a}	MS/RI	24.00	1303.74	1360	coconut, creamy, waxy, buttery	0.71
52		1117-52-8	Farnesyl acetone	$C_{18}H_{30}O$	–	–	–	–	14.18 ± 1.07^{b}	19.56 ± 3.53^{a}	MS/RI	36.60	1918.36	1915	flower	0.50
53		1072–83-9	2-Pyrrolyl methyl ketone	C_6H_7NO	–	–	–	–	40.65 ± 2.29^{b}	305.35 ± 1.75^{a}	MS/RI	15.32	1064.24	1063.2	nut, cherry, walnut, bready	1.83
54		930–60-9	4-Cyclopentene-1,3-dione	$C_5H_4O_2$	–	–	–	–	–	15.02 ± 5.08^{a}	MS/RI	8.91	883.84	880	N	0.44
55		1193-18-6	3-Methyl-2-cyclohexen-1-one	$C_7H_{10}O$	–	–	–	–	–	2.55 ± 0.75^{a}	MS/RI	14.08	1027.39	1026	nut, caramel, cherry	0.19
56		693–54-9	2-Decanone	$C_{10}H_{20}O$	–	–	–	–	–	13.63 ± 3.31^{a}	MS/RI	19.26	1189.50	1191	orange, floral, fatty, peach	0.42
57		3188-00-9	Dihydro-2-methyl-3-furanone	$C_5H_8O_2$	–	–	–	–	–	1.00 ± 0.64^{a}	MS/RI	5.96	803.36	804	sweet, bread, buttery, nutty	0.60
58		122–57-6	4-Phenylbutenone	$C_{10}H_{10}O$	–	–	–	–	–	7.48 ± 1.75^{a}	MS/RI	23.88	1393.30	1346	sweet, spice, cinnamon, creamy, floral	0.31
59		2922-51-2	2-Heptadecanone	$C_{17}H_{34}O$	–	–	–	–	–	5.78 ± 2.64^{a}	MS/RI	36.24	1893.67	1897	N	0.28
60	**Others**	13,679–41-9	3-phenyl-Furan	$C_{10}H_8O$	5.25 ± 0.56^{c}	–	12.58 ± 5.08^{c}	13.66 ± 5.38^{c}	36.37 ± 3.45^{b}	33.86 ± 3.97^{a}	MS/RI	20.10	1217.99	1226.8	N	0.66
61		3482-63-1	1-methoxy-Dodecane	$C_{13}H_{28}O$	3.67 ± 0.78^{c}	5.46 ± 2.45^{c}	6.49 ± 2.75^{c}	12.71 ± 3.05^{c}	9.39 ± 1.23^{b}	10.56 ± 1.31^{a}	MS/RI	25.66	1422.55	1424.1	N	0.47
62		18,679–18-0	(*Z*)-dihydro-5-(2-octenyl) furan-2(3H)-one	$C_{12}H_{20}O_2$	34.71 ± 4.56^{b}	42.52 ± 3.01^{b}	33.89 ± 3.31^{b}	59.05 ± 3.61^{b}	27.17 ± 4.67^{b}	108.33 ± 4.53^{a}	MS/RI	31.12	1691.71	1661	sweet, dairy, creamy, fruity	1.14
63		22,047–25-2	Acetylpyrazine	$C_6H_6N_2O$	–	–	–	4.26 ± 1.94^{b}	14.75 ± 4.67^{b}	15.89 ± 3.83^{a}	MS/RI	13.82	1019.41	1021	popcorn, nutty, chocolate, hazelnut, coffee	0.50
64		13,925–09-2	2-ethenyl-6-methyl-Pyrazine	$C_7H_8N_2$	–	–	–	–	28.96 ± 5.16^{b}	86.24 ± 2.05^{a}	MS/RI	13.57	1012.18	1016	N	0.69
65		1008–88-4	3-phenyl-Pyridine	$C_{11}H_9N$	–	–	–	–	12.47 ± 3.16^{b}	22.88 ± 5.38^{a}	MS/RI	26.55	1458.01	1470	N	0.47
66		123–32-0	2,5-dimethyl-Pyrazine	$C_6H_8N_2$	–	–	–	–	9.45 ± 1.05^{b}	39.86 ± 3.05^{a}	MS/RI	9.86	915.52	913	cocoa, roasted, nuts, roast, grass	0.64
67		109–08-0	methyl-Pyrazine	$C_5H_6N_2$	–	–	–	–	–	17.53 ± 3.61^{a}	MS/RI	6.51	818.21	826	nutty, roasted, chocolate, peanut	0.48

(*continued on next page*)

Table 1 (*continued*)

No.	Classification	CAS	Compounds	Formula	Content (μg/kg)						Identification Method	RT	RI [a]	RI [b]	Odor description	VIP
					0 h	1 h	3 h	5 h	7 h	9 h						
68		636–41-9	2-methyl-1H-Pyrrole	C_5H_7N	–	–	–	–	–	0.32 ± 0.04[a]	MS/RI	7.28	839.41	839	N	0.07
69		5910-89-4	2,3-dimethyl-Pyrazine	$C_6H_8N_2$	–	–	–	–	–	9.28 ± 2.05[a]	MS/RI	10.06	924.18	920	nut, cocoa, peanut, butter, walnut, caramellic	0.35
70		4177-16-6	ethenyl-Pyrazine	$C_6H_6N_2$	–	–	–	–	–	7.12 ± 1.94[a]	MS/RI	10.49	942.45	940	nutty	0.30
71		3658-80-8	Dimethyl trisulfide	$C_2H_6S_3$	–	–	–	–	–	5.42 ± 0.27[a]	MS/RI	11.83	1003.20	977.2	sulfurous, cooked, onion, savory, meaty	0.26
72		13,925–03-6	2-ethyl-6-methyl-Pyrazine	$C_7H_{10}N_2$	–	–	–	–	–	38.84 ± 1.61[a]	MS/RI	12.94	1079.88	1001	roasted, potato	0.71
73		13,360–64-0	2-ethyl-5-methyl-Pyrazine	$C_7H_{10}N_2$	–	–	–	–	–	16.74 ± 4.83[a]	MS/RI	13.04	1088.36	1025	bean, nutty, grassy, roasted	0.46
74		14,667–55-1	trimethyl-Pyrazine	$C_7H_{10}N_2$	–	–	–	–	–	26.81 ± 2.34[a]	MS/RI	13.09	1092.99	1020	nut, earthy, cocoa, potato, roasted	0.59
75		13,360–65-1	3-ethyl-2,5-dimethyl-Pyrazine	$C_8H_{12}N_2$	–	–	–	–	–	85.04 ± 2.34[a]	MS/RI	15.71	1075.83	1078	potato, cocoa, roasted, nutty	1.06
76		15,707–34-3	2,3-Dimethyl-5-ethylpyrazine	$C_8H_{12}N_2$	–	–	–	–	–	40.31 ± 3.61[a]	MS/RI	15.95	1083.23	1089	burnt, popcorn, roasted, cocoa	0.73
77		18,138–05-1	3,5-diethyl-2-methyl-Pyrazine	$C_9H_{14}N_2$	–	–	–	–	–	13.71 ± 1.94[a]	MS/RI	18.21	1155.07	1162	nutty, meaty, vegetable	0.42
78		17,398–16-2	2,3,5-Trimethyl-6-ethylpyrazine	$C_9H_{14}N_2$	–	–	–	–	–	15.97 ± 5.05[a]	MS/RI	18.30	1158.11	1155	N	0.46
79		91,010–41-2	2-Isoamyl-6-methylpyrazine	$C_{10}H_{16}N_2$	–	–	–	–	–	17.45 ± 2.94[a]	MS/RI	20.91	1246.58	1248	N	0.49
80		18,433–98-2	2,5-dimethyl-3-(3-methylbutyl)-Pyrazine	$C_{11}H_{18}N_2$	–	–	–	–	–	34.46 ± 2.47[a]	MS/RI	22.75	1320.66	1321	fruity	0.68

Note: RT, retention time (min); RI [a], retention index calculated; RI [b], retention index from the NIST webbook database; Odor description from http://www.perflavory.com/; N, not found in database; "-", not found in the sample. The superscript letters indicate a significant difference at the 0.05 significance level ($P < 0.05$).

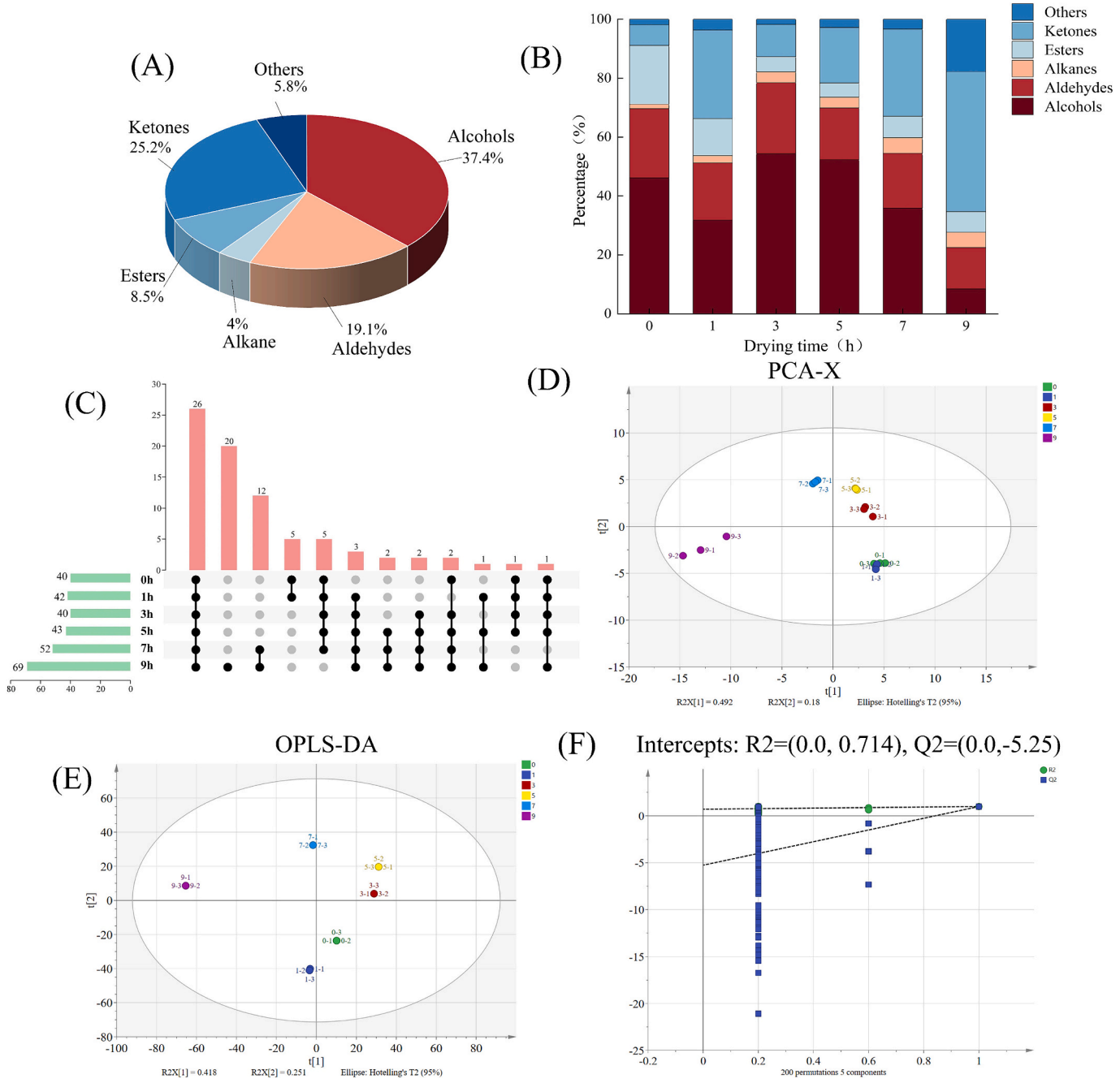

Fig. 2. Volatile compounds composition and multivariate analysis. (A) Proportion of different classes of volatile compounds; (B) The proportions of each category of volatile components at different drying stages. (C) Upset diagrams with volatile components at different drying stages. (D) Results of PCA-X analysis; (E) Results of OPLS-DA analysis; (F) Cross-validation plot by 200 permutation tests (R2 = 0.714, Q2 = −5.25).

activity of LOX was significantly higher than that of ADH. This provided an ample supply of precursors for the synthesis of aldehydes, which was one of the reasons for the overall higher contents of aldehydes in the *Boletus edulis*. The enzymatic activities of γ-GGT and C—S lyase both reached their maximum values at 3 h, and with prolonged drying time, their activities exhibited a trend of initial decrease followed by an increase. Combining the results from HS-SPME/GC–MS, it was observed that the content of sulfur-containing compounds showed an initial increase followed by a decrease during the drying process, reaching its peak at 9 h. It was hypothesized that the γ-GGT and C—S lyase were activated around 3 h of drying, and the content of sulfur-containing compounds changed in tandem with enzymatic activities, leading to the formation of 2-thiophenecarboxaldehyde, dimethyl trisulfide and methional. The 2-thiophenecarboxaldehyde typically exhibited peculiar fragrances, accompanied by unpleasant odors such as sourness and sulfur, while methional was characterized by a faint sweetness, and a subtle peppery flavor (Wang et al., 2023).

3.1.4. *The volatile components analyzed by correlation*

In order to directly reflect the differences in the content of volatile components in different drying stages of *Boletus edulis*, a cluster heatmap was constructed and analyzed for C-8 compounds and sulfur-containing compounds. As shown in Fig. 3C, hierarchal clustering of the volatile components profile during the drying process was performed. There were two main clusters in the pattern of volatile components accumulation. Significant accumulations of (E)-2-octen-1-ol and 1-octen-3-ol

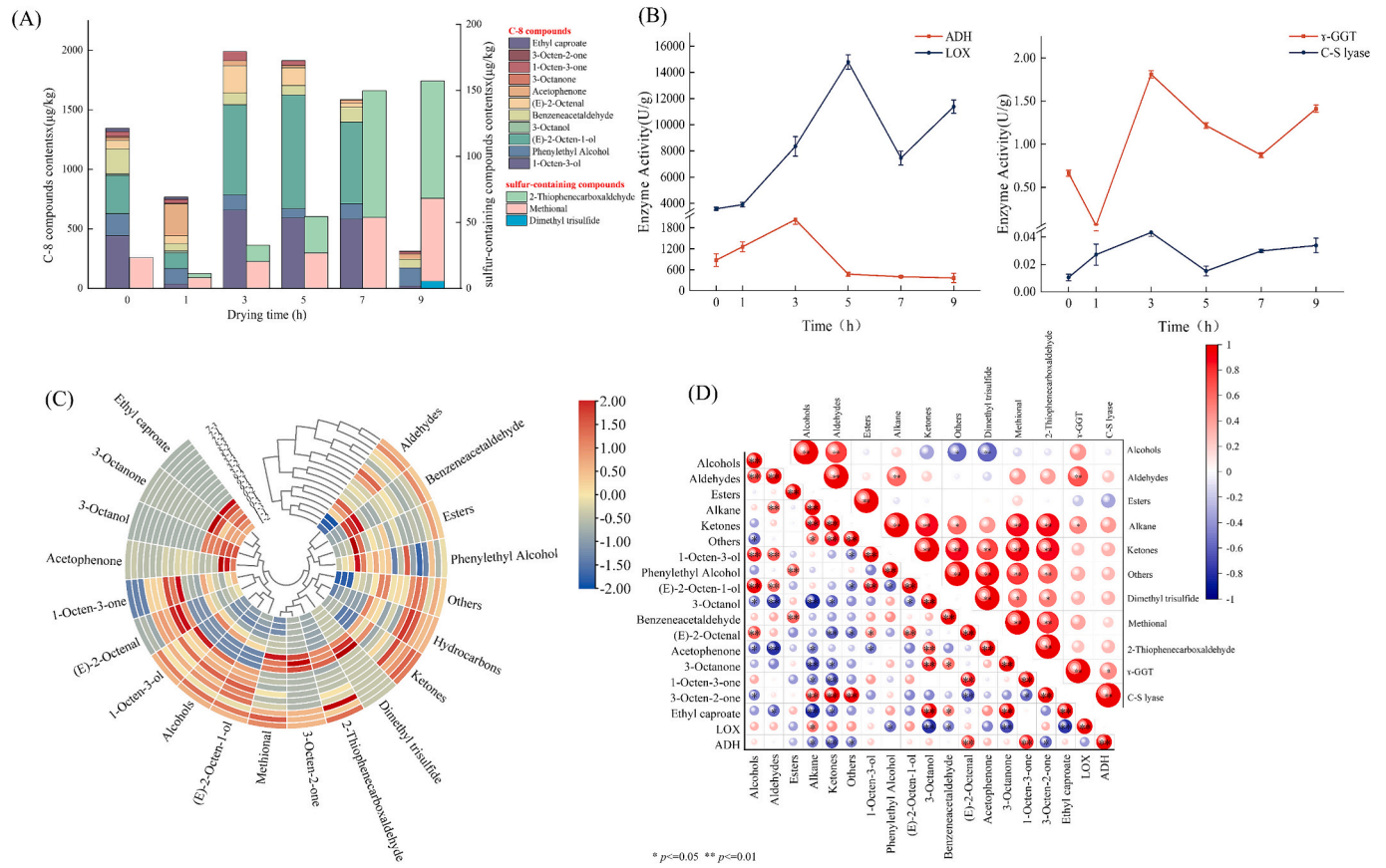

Fig. 3. Analysis of key enzyme activities during the drying process of *Boletus edulis*. (A) The categories and contents of C-8 compounds and sulfur-containing compounds during the drying processes; (B) Enzyme activity of ADH, LOX, γ-GGT and C—S lyase during the drying process; (C) Cluster analysis heat map of volatile flavor compounds; (D) Heatmap of Pearson's correlation analysis.

were observed during the initial and intermediate phases (0 h, 1 h, 3 h, 5 h) of the drying process. Furthermore, significant accumulations of phenylethyl alcohol, ketones, aldehydes and others were observed at 7 h and 9 h of the drying process. However, among the C-8 compounds, alcohols, ketones, and aldehydes were the volatile components that showed significant accumulations during the drying process. Alcohol compounds were primarily downstream products of lipid oxidation, which occurred under the action of a series of enzymes, mainly derived from polyunsaturated fatty acids. They are a class of volatile compounds with relatively high thresholds, contributing to flavor only when present in sufficient quantities (Li et al., 2019). Aldehyde compounds were mainly derived from the degradation of branched-chain and aromatic amino acids or cysteine, as well as the oxidative decomposition of unsaturated fatty acids (Hou et al., 2021). These results indicated that volatile components largely accumulated during the drying process. The differentially expressed volatile components may be important factors in aroma formation during the drying process.

Therefore, we focused on the analysis of the correlation among C-8 compounds, sulfur-containing compounds and the enzymatic activities of key flavor synthesis enzymes, and the results were illustrated in Fig. 3D. In conjunction with the enzyme activity results and HS-SPME/GC–MS findings, among the detected C-8 compounds, 1-octen-3-ol, phenylethyl alcohol, (E)-2-octen-1-ol, benzeneacetaldehyde, (E)-2-octenal, acetophenone, 1-octen-3-one and 2-thiophenecarboxaldehyde exhibited VIP values exceeding 1, indicating their significant relevance in elucidating the mechanisms of aroma formation during the drying process of flavorful *Boletus edulis*. These eleven C-8 compounds (1-octen-3-ol, phenylethyl alcohol, (E)-2-octen-1-ol, 3-octanol, benzeneacetaldehyde, (E)-2-octenal, ethyl caproate, acetophenone, 3-octanone, 1-octen-3-one and 3-octen-2-one) exhibited a marked positive correlation with LOX and ADH. Combining Fig. 3C and Fig. 3D, it can be observed that these C-8 compounds were significantly accumulated in samples (0 h, 1 h, 3 h, 5 h), which laid the foundation for the mushroom and floral aroma characteristics in the flavor profile of *Boletus edulis*. That suggesting the participation of LOX and ADH in enzymatic reactions that facilitated the generation of C-8 compounds and the development of distinctive flavors. Sulfur-containing compounds are typically derived from the thermal decomposition of sulfur-containing amino acids. 2-thiophenecarboxaldehyde, dimethyl trisulfide and methional exhibited a positive correlation with γ-GGT and C—S lyase, and γ-GGT and C—S lyase respectively underwent secondary activation during the drying stages at 7 h and 5 h, and these sulfur-containing compounds were significantly accumulated in samples (7 h, 9 h). That indicating that the enzymatic activity markedly influenced the generation of sulfur-containing compounds. Negative correlations or positive correlations were found between alkanes and enzyme activities, indicating that γ-GGT and LOX taking part in the early stages of the synthetic pathway of volatile components. ADH and C—S lyase contributed to the later stages of the synthetic pathway of volatile components, and have a strong correlation with the levels of the volatile end products. Most compounds demonstrated a noteworthy positive correlation, aligning with the findings in results of PCA-X and OPLS-DA analysis. This suggested that the drying treatment resulted in an augmentation of volatile compound content.

3.2. The non-volatile metabolites profile of boletus edulis by UPLC-MS/MS

3.2.1. Nontargeted metabolites analysis

The mass spectra total ion chromatograms (Base Peak) of QC samples

in positive and negative ion detection modes were respectively compared. The results indicated that the response intensities and retention times of each chromatographic peak were generally consistent. This suggested that throughout the entire experimental process, the variation caused by instrumental errors was minimal, and the data quality was reliable. In addition, the Pearson's correlation coefficients of each sample exceeded 0.9, indicating that the replicates within the group had strong correlation, good repeatability and good sample homogeneity, and thus could be used for subsequent different metabolites analysis. After data collation, 1319 non-volatile compounds were identified in the six samples, including 18 alkaloids and derivatives, 5 benzene and substituted derivatives, 155 benzenoids, 273 lipids and lipid-like molecules, 57 nucleosides, nucleotides, and analogues, 264 organic acids and derivatives, 26 organic nitrogen compounds, 115 organic oxygen compounds, 267 organoheterocyclic compounds, 91phenylpropanoids and polyketides and 48 others. (Table S1).

Principal component analysis (PCA) is a method used to illustrate overall metabolic differences between groups and the variation within each group. As shown in Fig. 4A, it can be seen from the chart that all samples were within a 95% confidence interval. The first principal component PC1 was 27.8%, and the second principal component PC2 was 15.3%, indicating that the extracted principal component factor can well explain the original variable information. There was a better separation trend observed in different drying stages, with the sample at 7 h positioned in the lower right quadrant of the coordinate axis, the sample at 9 h positioned in the upper right quadrant, and samples at 0 h, 1 h, and 3 h positioned on the left side of the coordinate axis, notably distant from the sample at 9 h. This result indicates that the metabolite content of *Boletus edulis* gradually changes during different drying processes.

3.2.2. *Metabolites analysis*

In the metabolite analysis, 479 differential metabolites were identified (Table S2). These differential metabolites mainly included organic acids and derivatives (20.88%), organoheterocyclic compounds (18.37%), lipids and lipid-like molecules (18.37%) and organic oxygen compounds (10.65%) (Fig. 4 B). As shown in Fig. 4C, a good clustering effect was observed for replicate samples within the same drying stage, and distinct separation was evident among different drying stages. This indicated that the accumulation of differential metabolites underwent dynamic changes across various drying stages of the boletus edulis, and the differences increased with the prolonged drying time.

Organic acids were an essential component of metabolism and could accelerate the conversion of polysaccharides and the breakdown of pectin substances (Hu, Feng, Ibrahim, & Liu, 2020). And organic acids could impart a refreshing and palatable taste. Among them, succinic acid was one of the most important by-products in the conversion of sugars to alcohol. Succinic acid was formed from malic acid under anaerobic conditions or the decomposition of certain amino acids (Wen et al., 2022). Similarly, succinic acid could also enhance the flavor of *Boletus edulis* by forming esters. Additionally, both succinic acid and citric acid were crucial substrates in the tricarboxylic acid (TCA) cycle. Amino acids were not only important for the regulation of human health but also played a significant role in the flavor and taste of *Boletus edulis*. Amino acids served as important precursors for flavor substances such as esters, higher alcohols, and pyrazines. Amino acids in *Boletus edulis* underwent metabolic breakdown into free amino acids, further generating carbonyl compounds, higher alcohols, and other flavor substances. For instance, cysteine and methionine, under the action of enzymes, formed sulfur-containing compounds that played a crucial role in the formation of *Boletus edulis* flavor (Wang et al., 2022). Leucine and phenylalanine were precursors for isoamyl alcohol and phenylethanol, respectively. Phenylalanine in the human body, when oxidized by hydroxylase, transformed into tyrosine, which could participate in the metabolism of fats and glucose.

Fatty acids and lipids were relevant structures and metabolic components of *Boletus edulis* cells, often serving as precursors to important volatile compounds. The β-oxidation of long-chain saturated fatty acids might have represented another biosynthetic pathway for aromatic compounds (Hou et al., 2024). Long-chain fatty acids were oxidized into short-chain acids such as acetic, butyric, and hexanoic acids, which were associated with the undesirable odors released by edible mushrooms. These short-chain acids underwent decarboxylation to form alcohols,

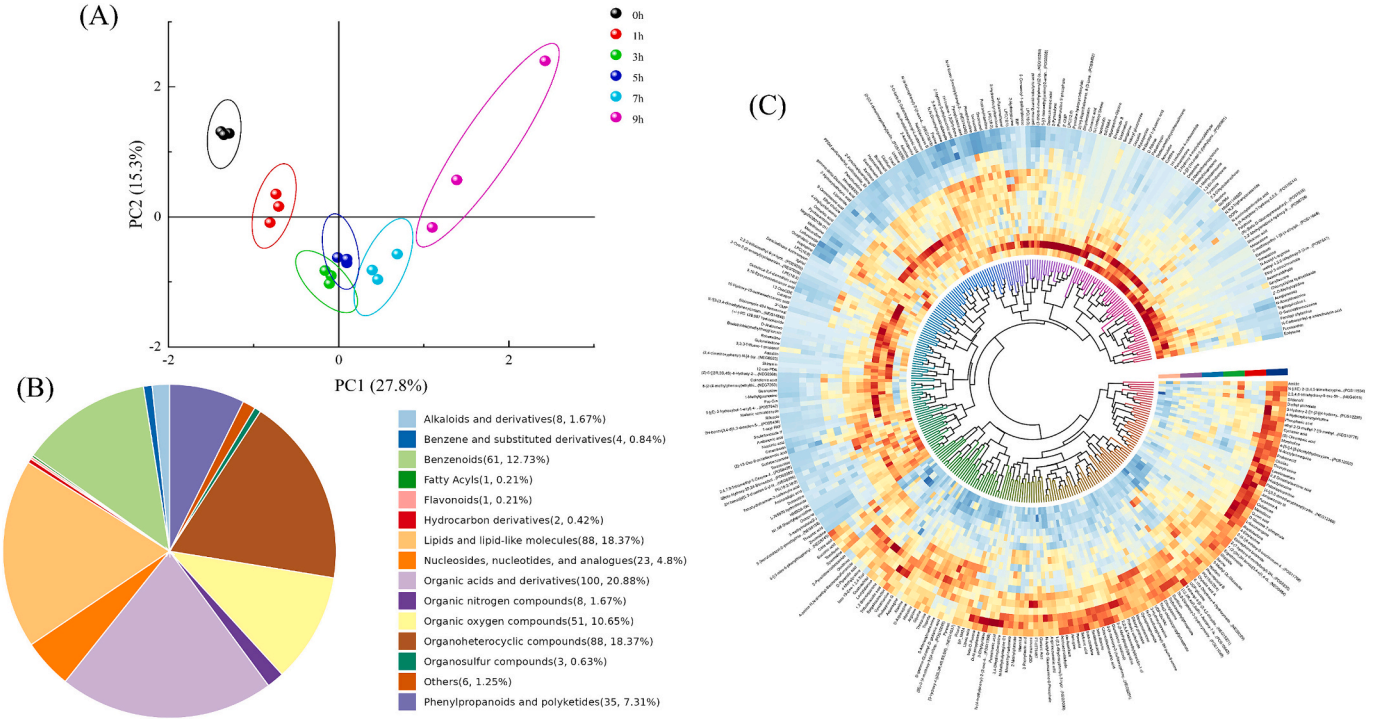

Fig. 4. Non-volatile compound composition and multivariate analysis. (A) PCA score of metabolites identified in *Boletus edulis*; (B) Pie chart of the biochemical categories of the non-volatile metabolites; (C) Heatmap of the changes in non-volatile metabolites.

which were esterified with acetyl-CoA via alcohol acyltransferase (AAT) to produce acetate esters (Espino-Diaz, & Sepúlveda1, D.R., González-Aguilar, G., & Olivas, G.I., 2016).

Various fatty acids and amino acids were catalytically transformed into a large number of volatile compounds as aromatic precursors under the action of certain enzymes. For example, C-8 compounds were typically generated from lipids catalyzed by LOX and HPL within the mushroom (Dickschat, 2017). These unsaturated fatty acids were first converted into hydrogen peroxide by LOX, then degraded into aldehydes by HPL. Subsequently, aldehydes were metabolized to alcohols by ADH (Li, 2021). And 1,2,4-trithiolane derived from the precursor γ-L-glutamylcysteinylglycine sulfoxide (*S*-methylmethionine) catalyzed by γ-GGT and C—S lyase, forming a sulfoxide intermediate (Li et al., 2021). The sulfoxide intermediate condensed and transformed into cyclic sulfur compounds. Additionally, cysteine was catalyzed by hydroxyproline oxidase (HPO), γ-GGT and C—S lyase to generate sulfur-containing flavor compounds such as 2-methyl-3-thiophenethiol, 2-thiophenecarboxaldehyde, dimethyl trisulfide and 2-butanone (Zhou, Kang, Yang, Song, & Liu, 2019). Furthermore, Methional was a volatile sulfur compound generated from methionine by the action of methionine lyase. Overall, the combination of these compounds collectively provided a distinctive flavor of *Boletus edulis*.

Carbohydrates present in mushrooms produced sweetness, serving as the main components determining the taste of edible fungi. Monosaccharides entered the TCA cycle through sugar fermentation pathways, producing organic acids and other compounds. Metabolism of carbohydrates resulted in the production of glycerol, butanediol, sorbitol, and other alcohols, enhancing sweetness (Heleno et al., 2011). Simultaneously, the alcohols and acids generated in this process contributed to the formation of important esters, contributing to the aroma of *Boletus edulis*.

3.2.3. *Differential metabolite screening and KEGG enrichment analysis*

Based on the VIP from the OPLS-DA model, combined with univariate analysis to screen for differential feature metabolites. A total of 479 differential metabolites with VIP > 1 and $P < 0.05$ were screened. As shown in Fig. 5, the differential metabolites were 473(1 h vs 0 h), 477(3 h vs 1 h), 396(5 h vs 3 h), 266(7 h vs 5 h), and 193 (9 h vs 7 h), respectively. Among these, 169 (1 h vs 0 h), 104 (3 h vs 1 h), 187 (5 h vs 3 h), 149 (7 h vs 5 h), and 141 (9 h vs 7 h) downregulated metabolites were identified, while 304 (1 h vs 0 h), 373 (3 h vs 1 h), 209 (5 h vs 3 h), 117 (7 h vs 5 h), and 52 (9 h vs 7 h) upregulated metabolites were screened. D-gamma-glutamyl-d-glutamic acid was downregulated in the 7 h vs 5 h and 9 h vs 7 h. According to the KEGG metabolic pathway description, D-gamma-Glutamyl-D-glutamic acid primarily participates in the metabolism of glutathione, and this substance is beneficial to the antioxidant system, capable of alleviating inflammation (Gao et al., 2022). Glutamic acid was upregulated in the 7 h sample. This substance participates in the biosynthesis of arginine, histidine metabolism, metabolism of arginine and proline, and metabolism of glutathione. It is an important precursor for synthesizing glutamine and proline (Azi et al., 2021). Compared to 1 h vs 0 h, 3 h vs 1 h and 5 h vs 3 h, fewer differential metabolites were produced at 9 h vs 7 h, indicating that *Boletus edulis* mainly generated abundant differential metabolites during the early-middle stage of drying. Furthermore, the total content of metabolites in the late drying stage was higher than in the early drying stage, indicating that with prolonged drying time, rich metabolites can be produced.

The enrichment analysis of metabolites through the metabolic pathways in the KEGG database facilitates the understanding of the mechanisms underlying metabolic pathway changes (Li et al., 2022). KEGG enrichment analysis (Fig. 6) further revealed that these differential metabolites were mainly classified into six pathways, which were metabolism pathway (M), environmental information processing pathway (E), organismal systems pathway (O), cellular processes pathway (C), human diseases pathway (H) and genetic information processing pathway (G). In the metabolism pathway, the most abundant pathways were amino acids metabolism pathway followed by nucleotide metabolism pathway, carbohydrate metabolism pathway and the metabolism pathway of cofactors and vitamins. Additionally, differential metabolites were predominantly annotated and enriched in the biosynthesis of amino acids, purine metabolism, pyrimidine metabolism, alanine, aspartate and glutamate metabolism, arginine and proline metabolism, cysteine and methionine metabolism, carbon

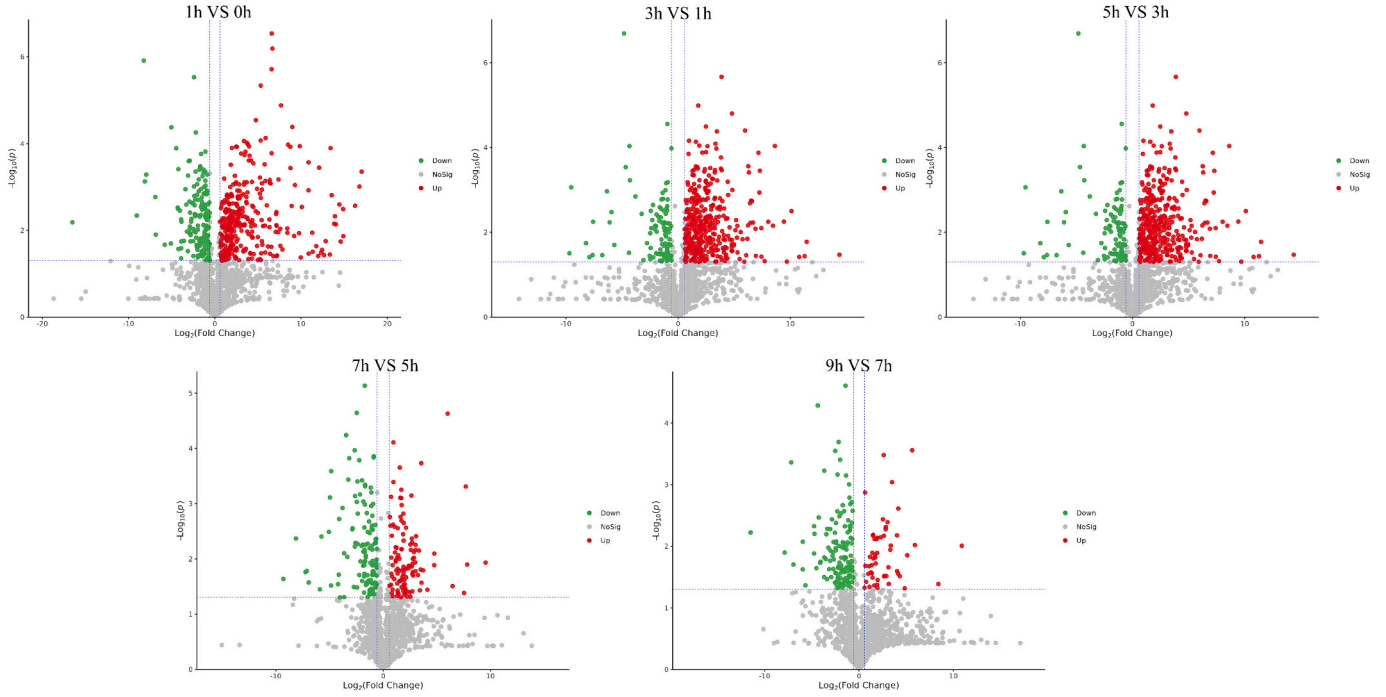

Fig. 5. Volcano plots of differential metabolites in *Boletus edulis*. The green dots represent down-accumulated differential metabolites, and the red dots represent up-accumulated differential metabolites. (For interpretation of the references to colour in this figure legend, the reader is referred to the web version of this article.)

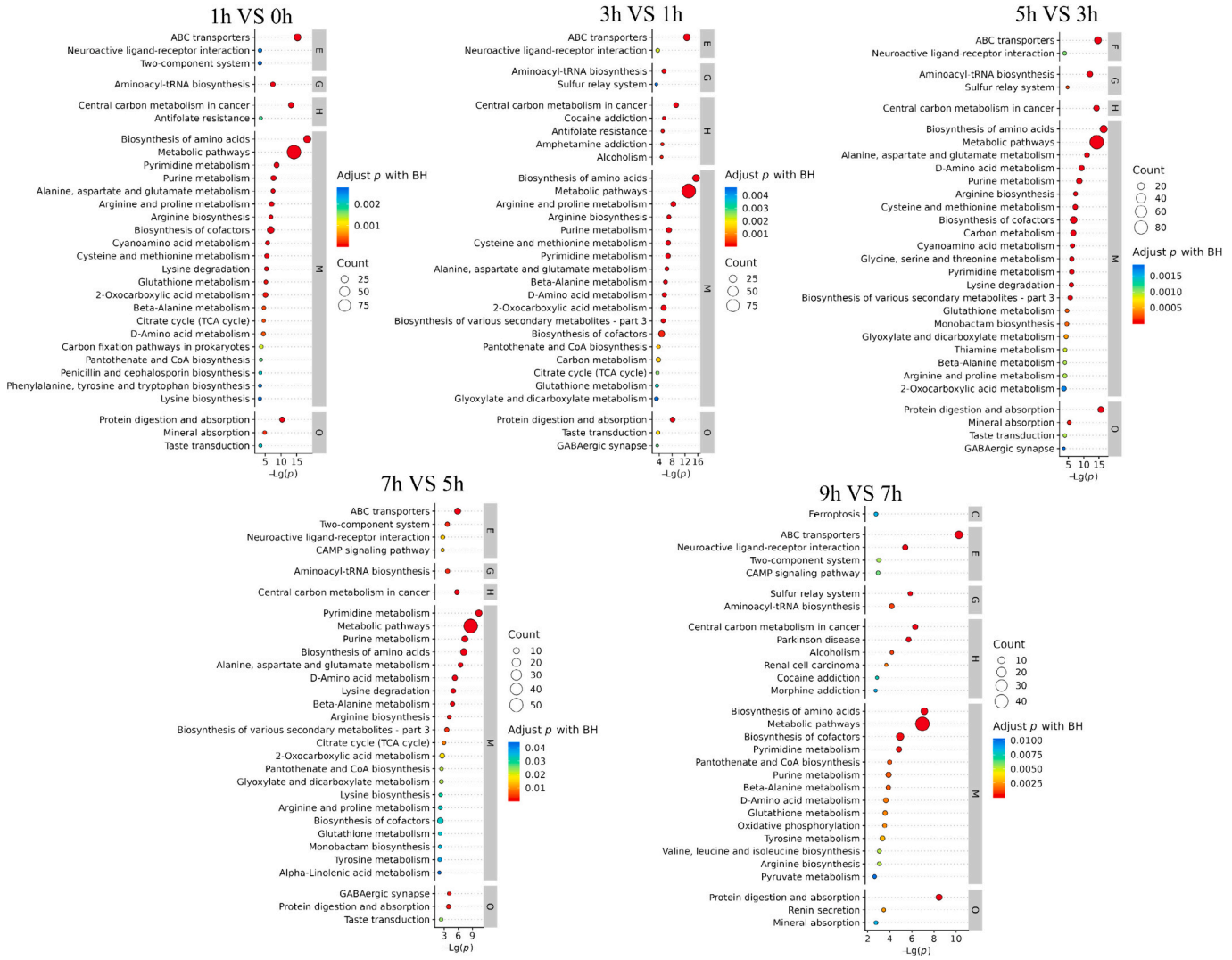

Fig. 6. The top 20 significantly enriched KEGG pathways of differential metabolites.

metabolism, glycine, serine, and threonine metabolism, glutathione metabolism, and biosynthesis of various secondary metabolites. Therefore, amino acids, carbohydrates and secondary metabolites may play a critical role in the flavor quality of *Boletus edulis*.

3.3. Metabolism pathway of cysteine, methionine and linoleic acid in boletus edulis

It was reported in the literature that linoleic acid and sulfur-containing amino acids are precursors of C-8 compounds and sulfur-containing compounds in edible mushrooms. However, What attracted us was that how were the metabolic pathways and metabolites of these flavor precursor formed at different drying stages. Therefore, we specifically focused on the metabolism of cysteine and methionine and the metabolism of linoleic acid. We hope these results provide new insights into the formation of flavor compounds during the drying process of delicious *Boletus edulis*. As shown in Fig. 7. L-Methionine was converted to S-Adenosylmethionine by S-adenosylmethionine synthetase, and S-Adenosylmethionine was catalyzed by methyltransferase and glycine *N*-methyltransferase to produce S-Adenosylhomocysteine. S-Adenosylhomocysteine was catalyzed by adenosylhomocysteine nucleosidase and adenosylhomocysteinase to respectively generate S-Ribosylhomocysteine and Homocysteine. Homocysteine was ultimately formed into L-Cysteine under the catalysis of relevant enzymes. These compounds were all formed into important precursors of sulfur-containing compounds, providing a solid foundation for the sulfur, onion, and meaty aroma of *Boletus edulis*. 8(*R*)-hydroperoxyoctadecadienoic acid, (9Z,11E)-13-Oxooctadeca-9,11-dienoic acid and (9S,10E,12Z)-9-Hydroperoxy-10,12-octadecadienoate were produced through the metabolism of linoleic acid, all showing accumulation with prolonged drying time, and significant accumulation at 5 h and 7 h. These compounds may further undergo cleavage into C-8 compounds under the action of LOX and ADH. Combining the results of GC–MS, it was observed that the detected C-8 compounds accumulated significantly at 5 h and 7 h, consistent with linoleic acid metabolites. This suggests that linoleic acid metabolism significantly contributes to the mushroom, earthy, and fruity aroma of *Boletus edulis*.

4. Conclusion

In this study, the changes in volatile components and non-volatile compounds in *Boletus edulis* at different drying stages were investigated by using HS-SPME-GC–MS and UPLC-MS/MS analysis methods. The results demonstrated that 80 volatile components and 1319 non-volatile compounds were identified in samples. Among volatile components, C-8 compounds and sulfur-containing compounds were of significant importance to the flavor of *Boletus edulis*. The correlation analysis results indicated that the formation of 1-octen-3-ol and other

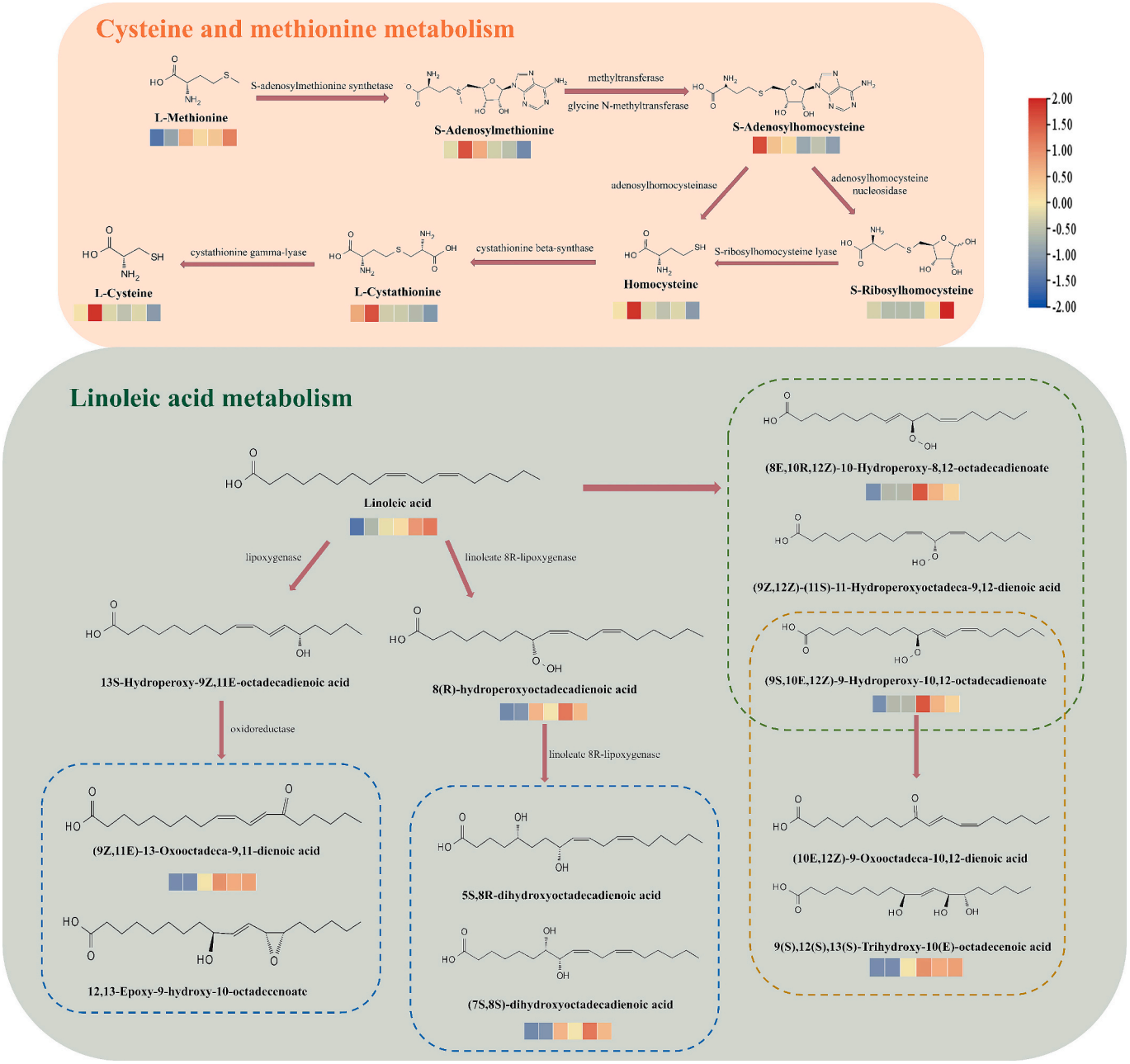

Fig. 7. The metabolic pathways of amino acids and fatty acids in different drying stages of *Boletus edulis*.The box of different colors represents the contents of metabolites (from left to right are 0 h, 1 h, 3 h, 5 h, 7 h, 9 h), where red and blue colors represent high and low level, respectively. (For interpretation of the references to colour in this figure legend, the reader is referred to the web version of this article.)

eight-carbon compounds was associated with LOX and ADH, while the formation of methional, 2-thiophenecarboxaldehyde, and dimethyl trisulfide was associated with γ-GGT and C—S lyase. Metabolomic analysis revealed that the metabolic pathways of metabolites primarily included amino acid metabolism, nucleotide metabolism, and carbohydrate metabolism. Differential metabolites were mainly annotated and enriched in the proline, aspartate, and glutamate metabolism, cysteine and methionine metabolism, glycine, serine, and threonine metabolism, glutathione metabolism, and the biogenesis of various secondary metabolites. As the drying time prolonged, the content of differential metabolites significantly accumulated in the later drying stages, generating abundant metabolites. And fatty acids, amino acids, and carbohydrates, serving as precursors, were catalytically transformed into volatile compounds under the specific enzymatic action, which significantly contributed to the flavor formation of *Boletus edulis*. This study provides novel evidence of metabolic profiles underlying flavor differences in the drying stages of *Boletus edulis*.

CRediT authorship contribution statement

Weilan Li: Writing – review & editing, Visualization, Formal analysis, Data curation. **Luxi Zi:** Methodology, Investigation. **Ningmeng Xu:** Visualization, Methodology, Investigation. **Zhengyin Guo:** Software, Data curation. **Bangjie Chen:** Formal analysis, Data curation. **Yan Hua:** Visualization, Software, Project administration. **Lei Guo:** Writing – review & editing, Supervision, Software, Resources, Project administration.

Declaration of competing interest

The authors declare that they have no known competing financial interests or personal relationships that could have appeared to influence the work reported in this paper.

Data availability

Data will be made available on request.

Acknowledgments

This work was financially supported by the National Natural Science Foundation of China (grant No.32260639) and the Yunnan Provincial Department of Science and Technology (grant No.202101AT070042 and grant No.202101BD070001-054).

Appendix A. Supplementary data

Supplementary data to this article can be found online at https://doi.org/10.1016/j.fochx.2024.101487.

References

Azi, F., Tu, C., Meng, L., Yu, Z. Y., Cherinet, M. T., Ahmadullah, Z., & Dong, M. S. (2021). Metabolite dynamics and phytochemistry of a soy whey-based beverage bio-transformed by water kefir consortium. *Food Chemistry, 342*, Article 128225. https://doi.org/10.1016/j.foodchem.2020.128225

Cebi, N. (2021). Quantification of the geranium essential oil, palmarosa essential oil and phenylethyl alcohol in *Rosa damascena* essential oil using ATR-FTIR spectroscopy combined with chemometrics. *Foods, 10*, 1848. https://doi.org/10.3390/foods10081848

Chen, D., Sheng, M. L., Wang, S. L., Chen, X. H., & Leng, A. X. (2023). Dynamic changes and formation of key contributing odorants with amino acids and reducing sugars as precursors in *shiitake* mushrooms during hot air drying. *Food Chemistry, 424*, Article 136409. https://doi.org/10.1016/j.foodchem.2023.136409

Dickschat, J. S. (2017). Fungal volatiles – A survey from edible mushrooms to moulds. *Natural Product Reports, 34*(3), 310–328. https://doi.org/10.1039/c7np00003k

Dong, H., Xian, Y. P., Xiao, Y. L., Zhu, L., & He, J. P. (2019). Development and comparison of single-step solid phase extraction and QuEChERS clean-up for the analysis of 7 mycotoxins in fruits and vegetables during storage by UHPLC-MS/MS. *Food Chemistry, 274*, 471–479. https://doi.org/10.1016/j.foodchem.2018.09.035

Espino-Diaz, M., & Sepúlveda1, D.R., González-Aguilar, G. & Olivas, G.I.. (2016). Biochemistry of apple aroma: A review. *Food Technology and Biotechnology, 54*(4), 375–394. https://doi.org/10.17113/ftb.54.04.16.4248

Gao, Y. X., Li, D. F., Tian, Z. L., Hou, L. Z., Gao, J., Fan, B., Wang, F. Z., & Li, S. Y. (2022). Metabolomics analysis of soymilk fermented by *Bacillus subtilis* BSNK-5 based on UHPLC-Triple-TOF-MS/MS. *LWT - Food Science and Technology, 160*, Article 113311. https://doi.org/10.1016/j.lwt.2022.113311

Heleno, S. A., Barros, L., Sousa, M. J., Martins, A., Buelga, S. C., & Ferreira, I. C. F. R. (2011). Targeted metabolites analysis in wild *boletus species*. *LWT - Food Science and Technology, 4*(6), 1343–1348. https://doi.org/10.1016/j.lwt.2011.01.017

Hou, H., Liu, C., Lu, X. S., Hu, Q. H., Zhang, Y. Y., & Zhao, L. Y. (2021). Characterization of flavor frame in shiitake mushrooms (*Lentinula edodes*) detected by HS-GC-IMS coupled with electronic tongue and sensory analysis: Influence of drying techniques. *LWT - Food Science and Technology, 146*, Article 111402. https://doi.org/10.1016/j.lwt.2021.111402

Hou, Z. S., Xia, R. R., Li, Y. T., Xu, H. R., Wang, Y. F., Feng, Y., Pan, S., Wang, Z. J., Ren, H. L., Qian, G. L., Wang, H. Y., Zhu, J. Y., & Xin, G. (2024). Key components, formation pathways, affecting factors, and emerging analytical strategies for edible mushrooms aroma: A review. *Food Chemistry, 438*, Article 137993. https://doi.org/10.1016/j.foodchem.2023.137993

Hu, S., Feng, W., Ibrahim, S. A., & Liu, Y. (2020). Effects of drying methods on non-volatile taste components of *Stropharia rugosoannulata* mushrooms. *LWT- Food Science and Technology, 127*, Article 109428. https://doi.org/10.1016/j.lwt.2020.109428

Li, J. L., Yang, Y., Li, W., Chen, W. C., & Liu, X. F. (2023). Aroma change and its relationship with key enzymatic reactions in drying process of Stropharia *rugosoannulata*. *Journal of Food Science and Technology, 41*(1), 20–42. https://doi.org/10.12301/spxb202200616

Li, R. (2021). *Research on formation mechanisms of characteristic aroma components of Lentinula edodes during drying process*. Lanzhou: Lanzhou University of Technology. https://doi.org/10.27206/d.cnki.ggsgu.2021.000723

Li, W., Chen, W. C., Wang, J. B., Feng, J., Wu, D., Zhang, Z., Zhang, J. S., & Yang, Y. (2021). Effects of enzymatic reaction on the generation of key aroma volatiles in *shiitake* mushroom at different cultivation substrates. *Food Science & Nutrition, 9*(4), 2247–2256. https://doi.org/10.1002/fsn3.2198

Li, W., Chen, W. C., Wu, D., Zhang, Z., Yang, Y., & Zhang, J. S. (2022). Understanding the promotion of heat treatment on the flavor of *Lentinula edodes* using metabolomics integrated with transcriptomics. *Food Research International, 162*, Article 112051. https://doi.org/10.1016/j.foodres.2022.112051

Li, W., Wang, J. B., Chen, W. C., Yang, Y., Zhang, J. S., Feng, J., Yu, H. L., & Li, Q. Z. (2019). Analysis of volatile compounds of *Lentinula edodes* grown in different culture substrate formulations. *Food Research International, 125*, Article 108517. https://doi.org/10.1016/j.foodres.2019.108517

Li, W. L., Zi, L. X., Xu, N. M., Huang, Z. F., Li, C. Y., & Guo, L. (2023). Effect of different vacuum drying temperature on the quality of *boletus edulis*. *Food Science and Technology, 48*(03), 35–44. https://doi.org/10.13684/j.cnki.spkj.2023.03.005

Magalhães, H. C. R., Filho, E. G. A., Meza, S. L. R., Oliveira, A., Garruti, D. S., & Purgatto, E. (2023). Effect of methyl Jasmonate on the biosynthesis of volatile compounds associated with the ripening of grape tomato fruits. *Journal of Agricultural and Food Chemistry, 71*(11), 4696–4705. https://doi.org/10.1021/acs.jafc.2c06215

Niu, W., Tian, H., & Zhan, P. (2022). The effects of pepper (*Zanthoxylum bungeanum*) from different production areas on the volatile flavor compounds of fried pepper oils based on HS-SPME–GC–MS and multivariate statistical method. *Molecules, 27*, 7760. https://doi.org/10.3390/molecules27227760

Qi, L., Gao, J. X., Xue, J., Chen, D., Lin, S. Y., Dong, X. P., & Zhu, B. W. (2020). Changes in aroma profile of shiitake mushroom (*Lentinus edodes*) during different stages of hot air drying. *Foods, 9*(4), 444. https://doi.org/10.3390/foods9040444

Ren, S. Y., Zheng, E. P., Zhao, T. X., Hu, S. Q., & Yang, H. L. (2022). Evaluation of physicochemical properties, equivalent umami concentration and antioxidant activity of *Coprinus comatus* prepared by different drying methods. *LWT-Food Science and Technology, 162*, Article 113479. https://doi.org/10.1016/j.lwt.2022.113479

Shakoor, A., Zhang, A., Xie, J. C., & Yang, X. L. (2022). Maillard reaction chemistry in formation of critical intermediates and flavor compounds and their antioxidant properties. *Food Chemistry, 393*, Article 133436. https://doi.org/10.1016/j.foodchem.2022.133416

Sun, L. B., Xin, G., Hou, Z. S., Zhao, X. M., Hu, H. R., Bao, X. J., Xiao, R. R., Li, Y. T., & Li, L. (2021). Biosynthetic mechanism of key volatile biomarkers of harvested *Lentinula edodes* triggered by spore release. *Journal of Agricultural and Food Chemistry, 69*(32), 9350–9361. https://doi.org/10.1021/acs.jafc.1c02410

Tan, Y. Q., Zeng, N. K., & Xu, B. J. (2022). Chemical profiles and health-promoting effects of porcini mushroom (*boletus edulis*): A narrative review. *Food Chemistry, 390*, Article 133199. https://doi.org/10.1016/j.foodchem.2022.133199

Tian, Y. T., Zhao, Y. T., Huang, J. J., Zeng, H. L., & Zheng, B. (2016). Effects of different drying methods on the product quality and volatile compounds of whole *shiitake* mushrooms. *Food Chemistry, 197*, 714–722. https://doi.org/10.1016/j.foodchem.2015.11.029

Tu, Z., Liu, Y. Y., Lin, J. Z., Lv, H. W., Zhou, W., Zhou, X. F., Qian, Y. F., Zeng, X., He, W. Z., & Ye, Y. (2023). Comparison of volatile and nonvolatile metabolites in green tea under hot-air drying and four heat-conduction drying patterns using widely targeted metabolomics. *Food Chemistry: X, 19*, Article 100767. https://doi.org/10.1016/j.fochx.2023.100767

Wang, B., Qu, F., Wang, P., Zhao, L., Wang, Z., Han, Y., & Zhang, X. (2022). Characterization analysis of flavor compounds in green teas at different drying temperature. *LWT-food science and technology, 161*, Article 113394. https://doi.org/10.1016/j.lwt.2022.113394

Wang, Q., Dong, K., Wu, Y. Y., An, F. P., Luo, Z., Huang, Q., & Wei, S. F. (2022). Exploring the formation mechanism of off-flavor of irradiated yak meat based on metabolomics. *Food Chemistry: X, 16*, Article 100494. https://doi.org/10.1016/j.fochx.2022.100494

Wang, Z., Kang, Q., Zhao, Y. H., Yan, R. Y., Sun, J. Y., Li, H. H., … Sun, B. G. (2023). Can the Maillard reaction affect the characteristic aroma of sesame aroma baijiu – A research on the methional during the stacking fermentation stage of jiupei. *Food Chemistry, 426*, Article 136521. https://doi.org/10.1016/j.foodchem.2023.136521

Wen, X. M., Li, W., Wu, L., Chen, W. C., Zhang, Z., Wu, D., & Yang, Y. (2022). Quality characteristics and non-volatile taste formation mechanism of *Lentinula edodes* during hot air drying. *Food Chemistry, 393*, Article 133378. https://doi.org/10.1016/j.foodchem.2022.133378

Zhang, H., Huang, D., Pu, D., Zhang, Y., Chen, H., Sun, B., & Ren, F. (2020). Multivariate relationships among sensory attributes and volatile components in commercial dry porcini mushrooms (*boletus edulis*). *Food Research International, 133*, Article 109112. https://doi.org/10.1016/j.foodres.2020.109112

Zhang, H. Y., Pu, D. D., Sun, B. G., Ren, F. Z., Zhang, Y. Y., & Chen, H. T. (2018). Characterization and comparison of key aroma compounds in raw and dry porcini mushroom (*boletus edulis*) by aroma extract dilution analysis, quantitation and aroma recombination experiments. *Food Chemistry, 258*, 260–268. https://doi.org/10.1016/j.foodchem.2018.03.056

Zhang, L., Hu, Y., Duan, X., Tang, T., Shen, Y., Hu, B., Liu, A., Chen, H., Li, C., & Liu, Y. (2018). Characterization and antioxidant activities of polysaccharides from thirteen boletus mushrooms. *International Journal of Biological Macromolecules, 113*, 1–7. https://doi.org/10.1016/j.ijbiomac.2018.02.084

Zhang, L. J., Dong, X. B., Feng, X., Ibrahim, S. A., Huang, W., & Liu, Y. (2021). Effects of drying process on the volatile and non-volatile flavor compounds of *Lentinula edodes*. *Foods, 10*, 2836. https://doi.org/10.3390/foods10112836

Zhang, Y. M., Li, X. B., Zhao, Z. Y., Chao, H., Fan, T. T., Dong, H., He, X. W., Zhao, X. Y., Tang, L. H., & Zhou, C. Y. (2023). Comprehensive investigation on non-volatile and volatile flavor compounds in the *Morchella sextelata* and *Morchella importuna* by UPLC-MS/ MS and GC × GC-TOF-MS. *Food Chemistry: X, 20*, Article 100961. https://doi.org/10.1016/j.fochx.2023.100961

Zhao, Z. Y., Fan, T. T., Chao, H., Zhang, Y. M., Li, X. B., Yang, X. L., Tian, E. J., Chen, A. L., Zhao, X. Y., & Zhou, C. Y. (2022). A simple derivatization method for simultaneous determination of four amino group-containing mushroom toxins in

mushroom and urine by UPLC-MS/MS. *Food Control, 137*, Article 108720. https://doi.org/10.1016/j.foodcont.2021.108720

Zhou, T. T., Kang, L., Yang, C., Song, H. L., & Liu, Y. (2019). Flavour precursor peptide from an enzymatic beef hydrolysate Maillard reaction-II: Mechanism of the synthesis of flavour compounds from a Sulphur-containing peptide through a Maillard reaction. *LWT - Food Science and Technology, 110*, 8–18. https://doi.org/10.1016/j.lwt.2019.04.022

Zhuang, J. D., Xiao, Q., Feng, T., Huang, Q. R., Ho, C. T., & Song, S. Q. (2020). Comparative flavor profile analysis of four different varieties of *boletus* mushrooms by instrumental and sensory techniques. *Food Research International, 136*, Article 109485. https://doi.org/10.1016/j.foodres.2020.109485